Karlsruher Institut für Technologie

Batterie- und Brennstoffzellensysteme

(Langzeit-) Stabilität von SOFC-Komponenten

André Weber

Institut für Werkstoffe der Elektrotechnik IWE
Adenauerring 20b, Geb. 50.40 (FZU), Raum 314
phone: 0721/608-7572, fax: 0721/608-7492
andre.weber@kit.edu
www.iwe.kit.edu

Institut für Werkstoffe der Elektrotechnik

Example
Activation and Degradation of an (La,Sr)(Mn,Co)O_3-Cathode

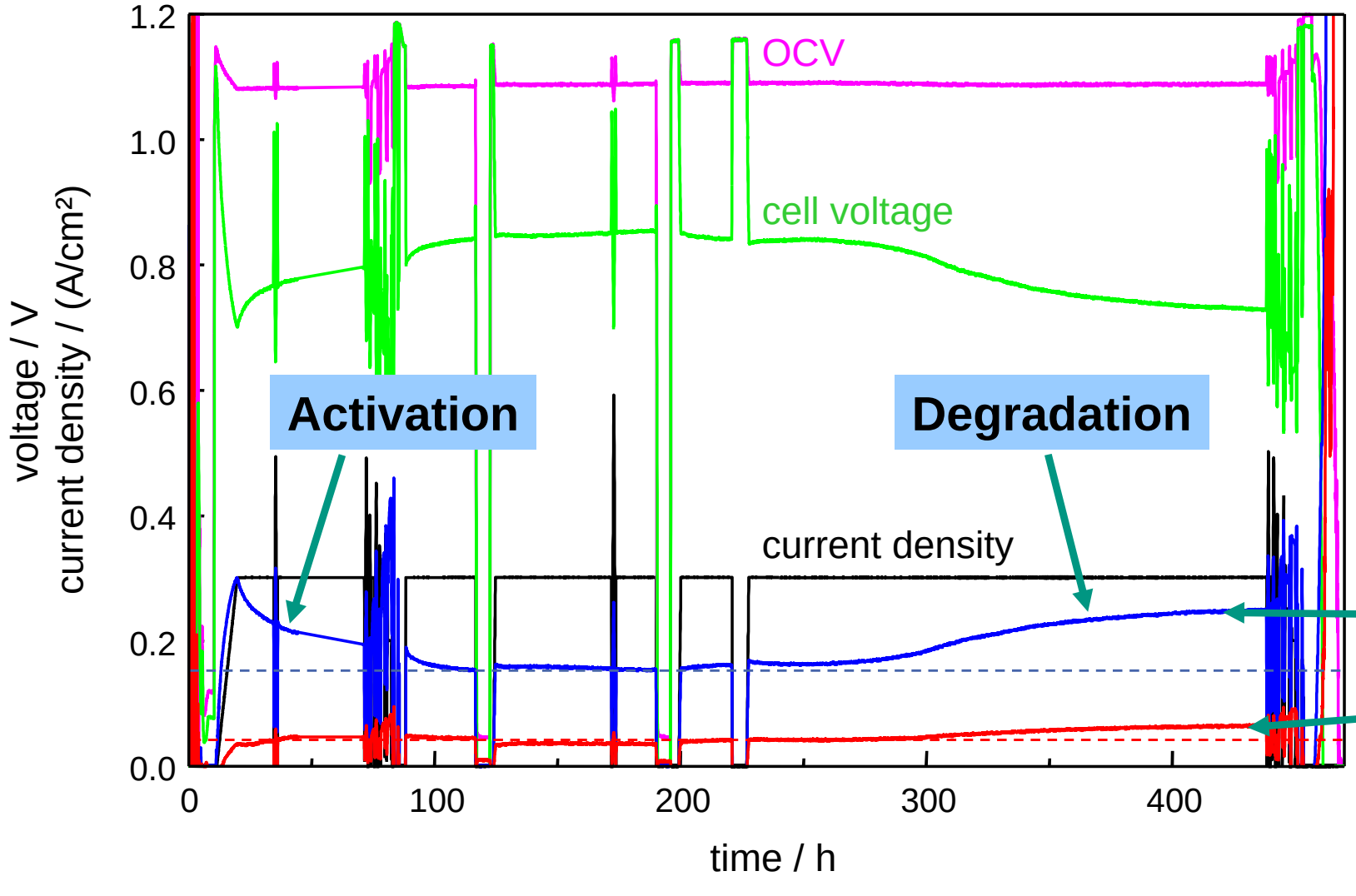

cell 3.3.2
cathode:
$La_{0.8}Ca_{0.2}Mn_{0.8}Co_{0.2}O_3$
electrolyte substrate (150 µm):
8 mol% Y_2O_3 dop. ZrO_2 (YSZ)
anode:
Ni/YSZ-Cermet
oxidant:
air, 0.5 slm
fuel:
H_2, 0.5 slm
temperature: 950 °C

Examples
Microstructural and chemical changes during operation

demixing and densification of the cathode

electrolyte de-mixing

intrinsic electrolyte degradation

Ni depletion at the interface

Ni agglomeration

delamination of the cathode layer

secondary phases at the interface

interdiffusion of cathode cations

interdiffusion of Ni

carbon and sulphur deposition

Kathode:
Formierung

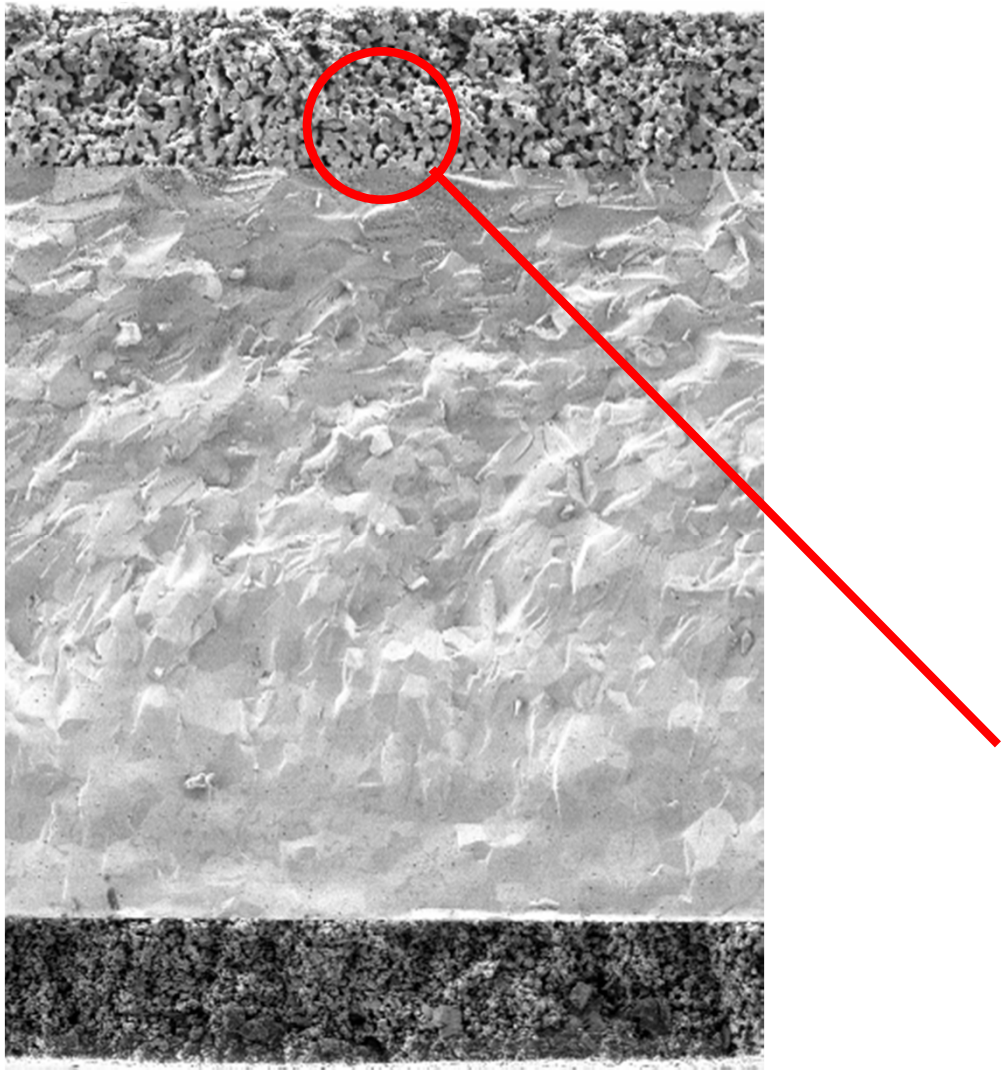

Cathode Degradation
Transport Processes

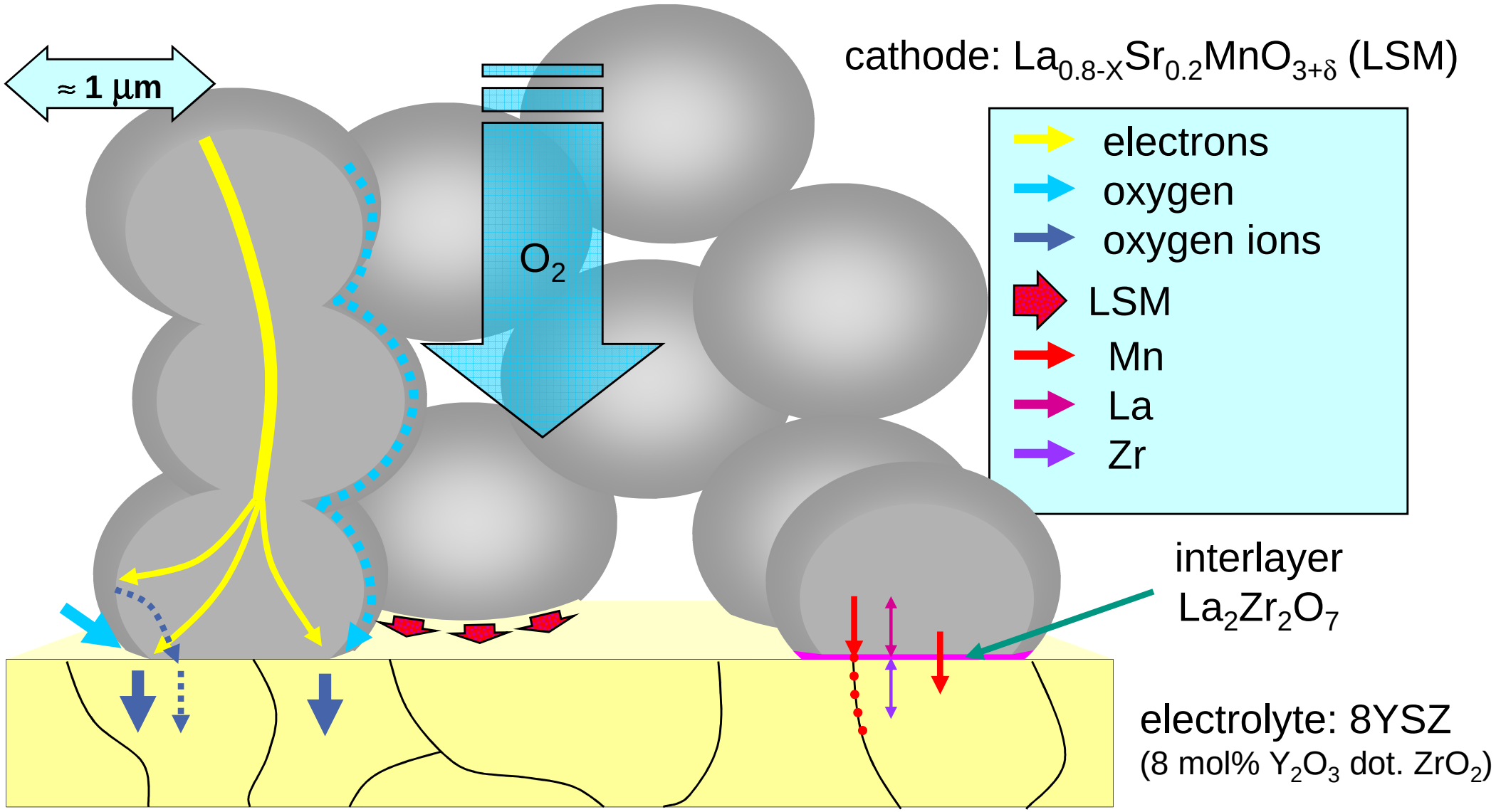

Startup Behavior of SOFC Single Cells and Stacks
Formation and Degradation

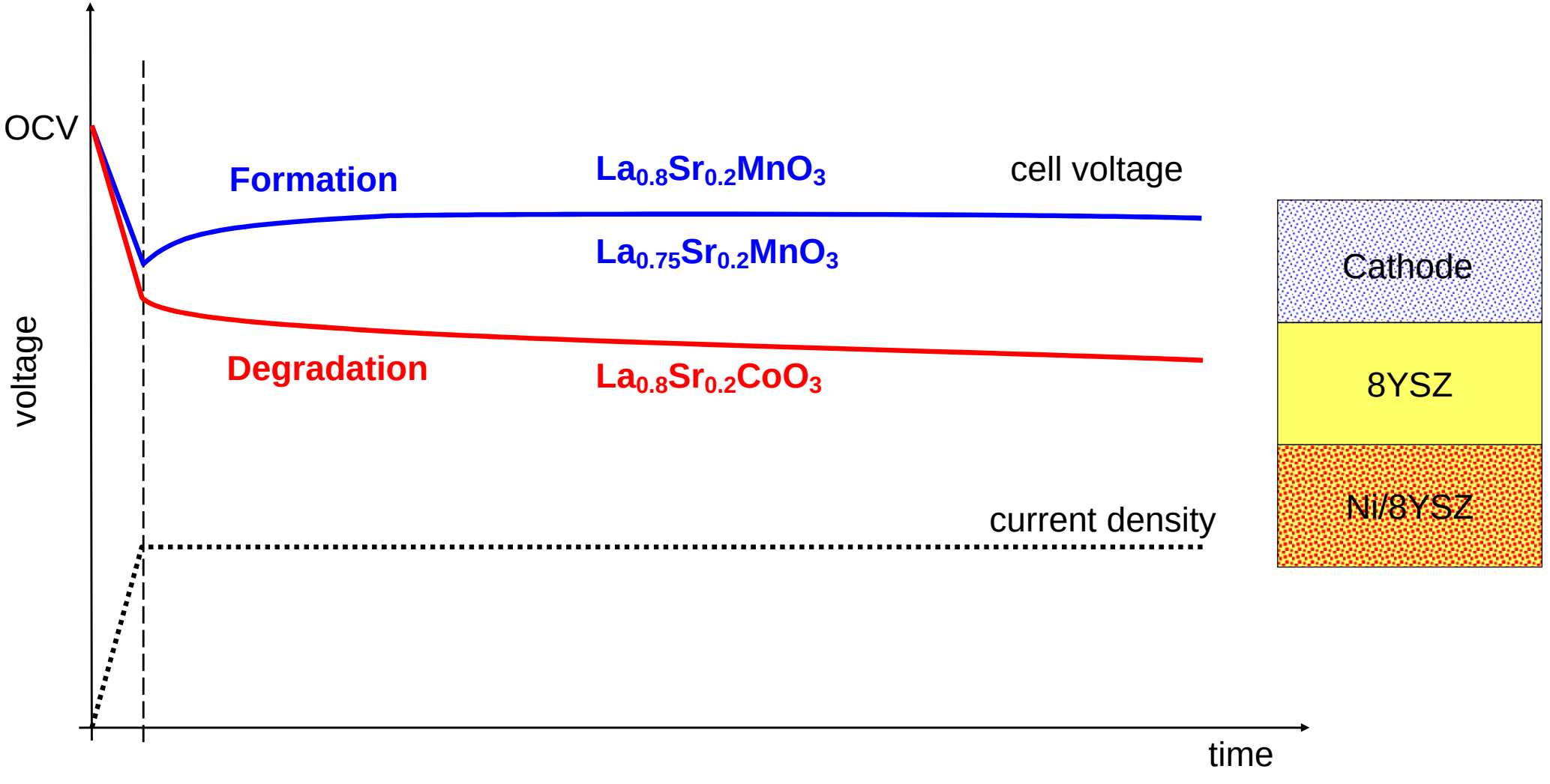

Cathode Degradation
Growth of Secondary Phases at the Cathode/Electrolyte-Interface

Interface LSM/8YSZ
(LSM: $La_{0.8}Sr_{0.2}MnO_{3+\delta}$)

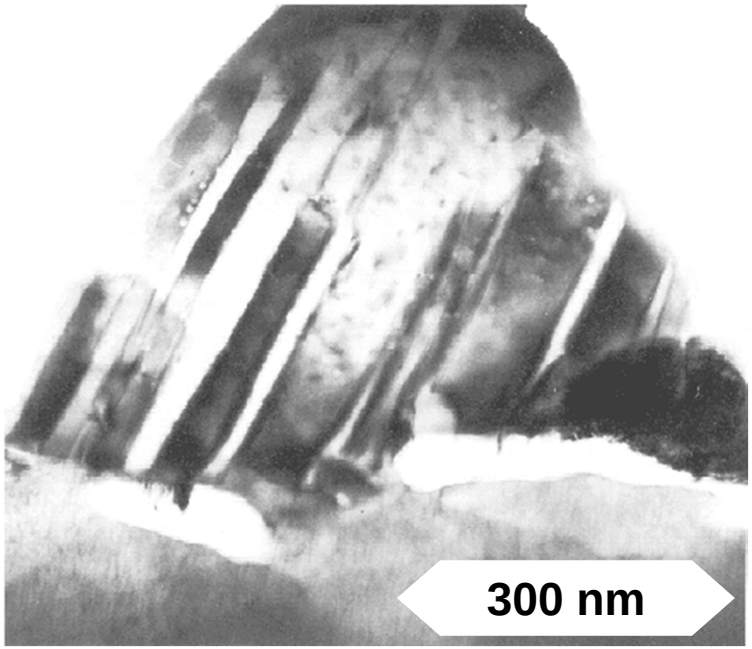

Interface LSMC/8YSZ
(LSMC: $La_{0.8}Sr_{0.2}Mn_{0.5}Co_{0.5}O_{3+\delta}$)

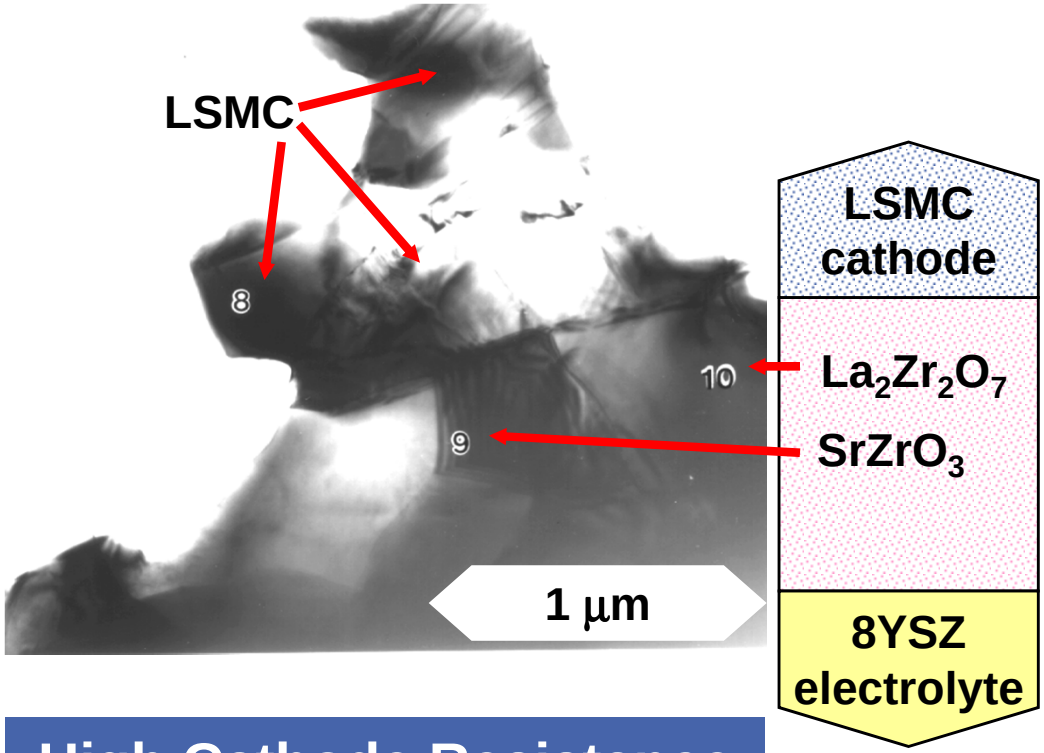

Decreased Cathode Resistance due to Formation

High Cathode Resistance due to Secondary Phases

SOFC: Formation and Long Term Test of a tubular Cell Siemens-Westinghouse SWPC (1997)

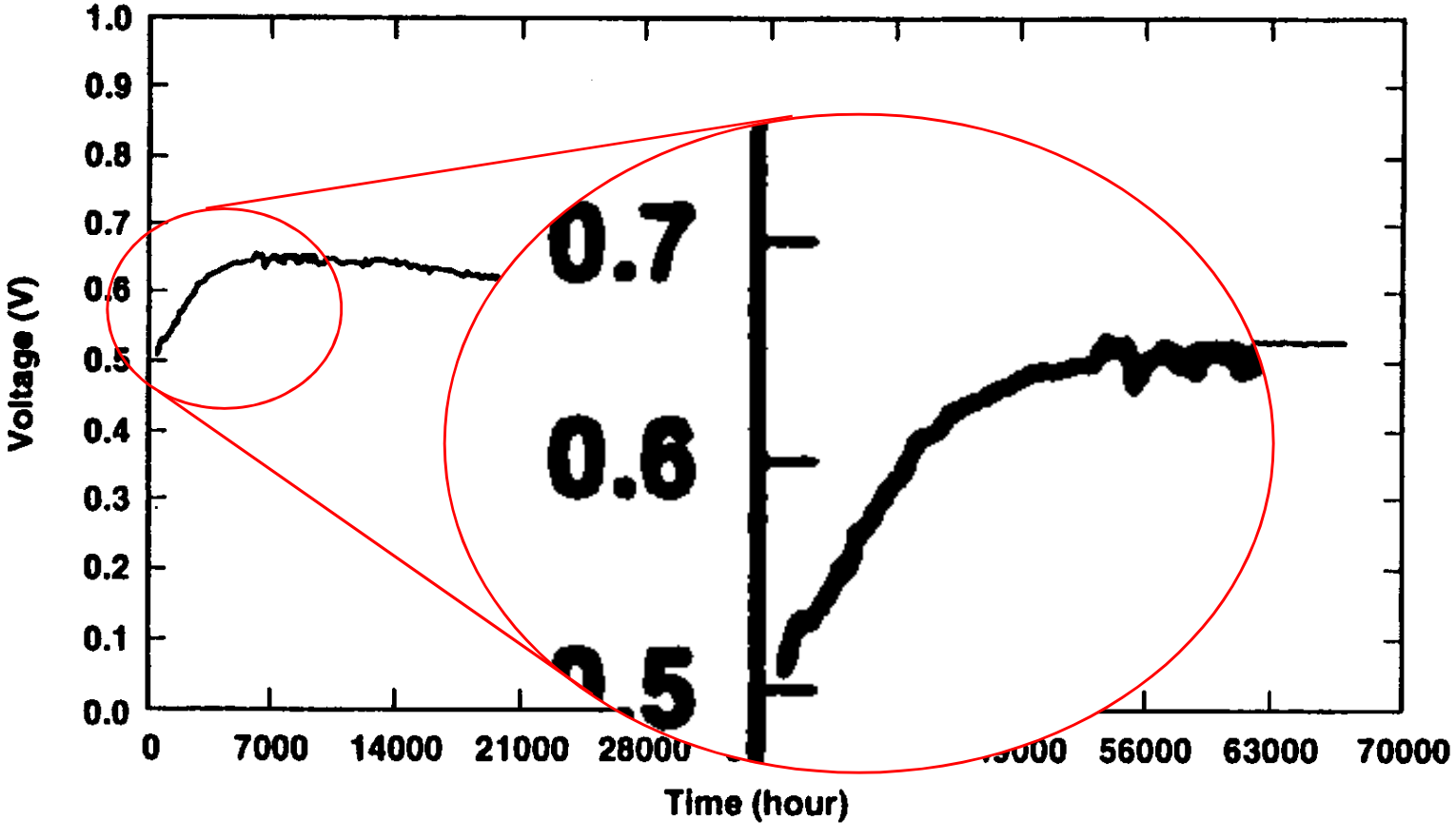

Fig. 1. Long term test of an early-technology PST cell.

V_{start} : 0.50 V

V_{max} : 0.65 V

► V_{max}: Point of max. performance

►time to V_{max} :

≈ 5.000 hours

S. C. Singhal, Recent Progress in Tubular Solid Oxide Fuel Cell Technology, Proc. 5th Int. Symposium on SOFC, Ed. U. Stimming, S. C. Singhal, H. Tagawa, W. Lehnert, The Electrochemical Society, PV 97-40, 37-50, (1997)

SOFC: Formation and Long Term Test of a 5-cell Stack Sulzer Hexis (1999)

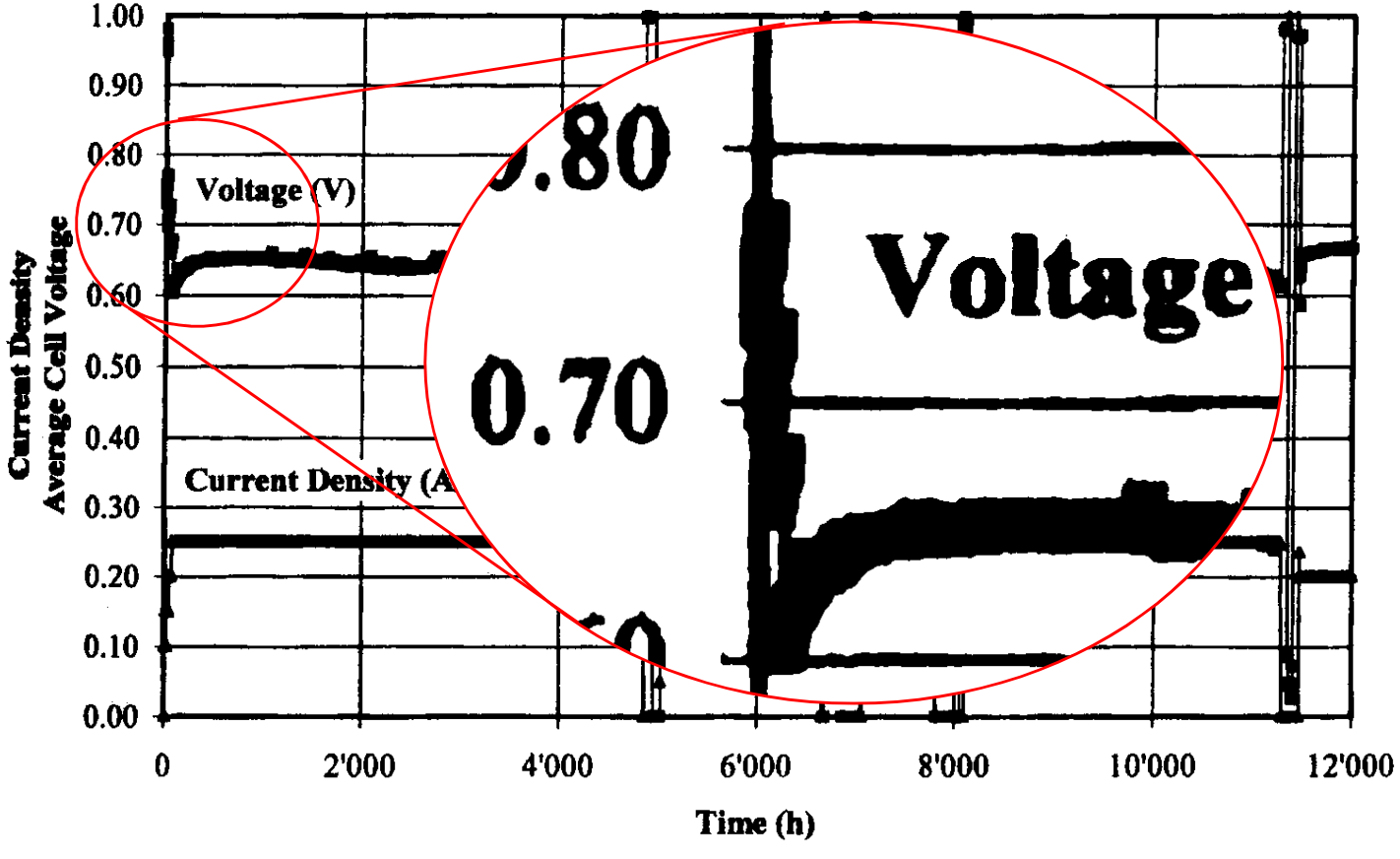

Figure 2: Negligible degradation of a five cell stack

V_{start} : 0.60 V

V_{max} : 0.65 V

► V_{max}: Point of max. performance

► time to V_{max} :

≈ 200 hours

R. Diethelm, M. Schmidt, Status of the Sulzer Hexis Product Development, Proc. 6th Int. Symp. on SOFC, Ed. S. Singhal und M. Dokiya, The Electrochemical Society, PV 99-19, 60-67, (1999)

SOFC: Formation and Long Term Test of a planar Cell Ceramic Fuel Cells Ld. CFCL (1999)

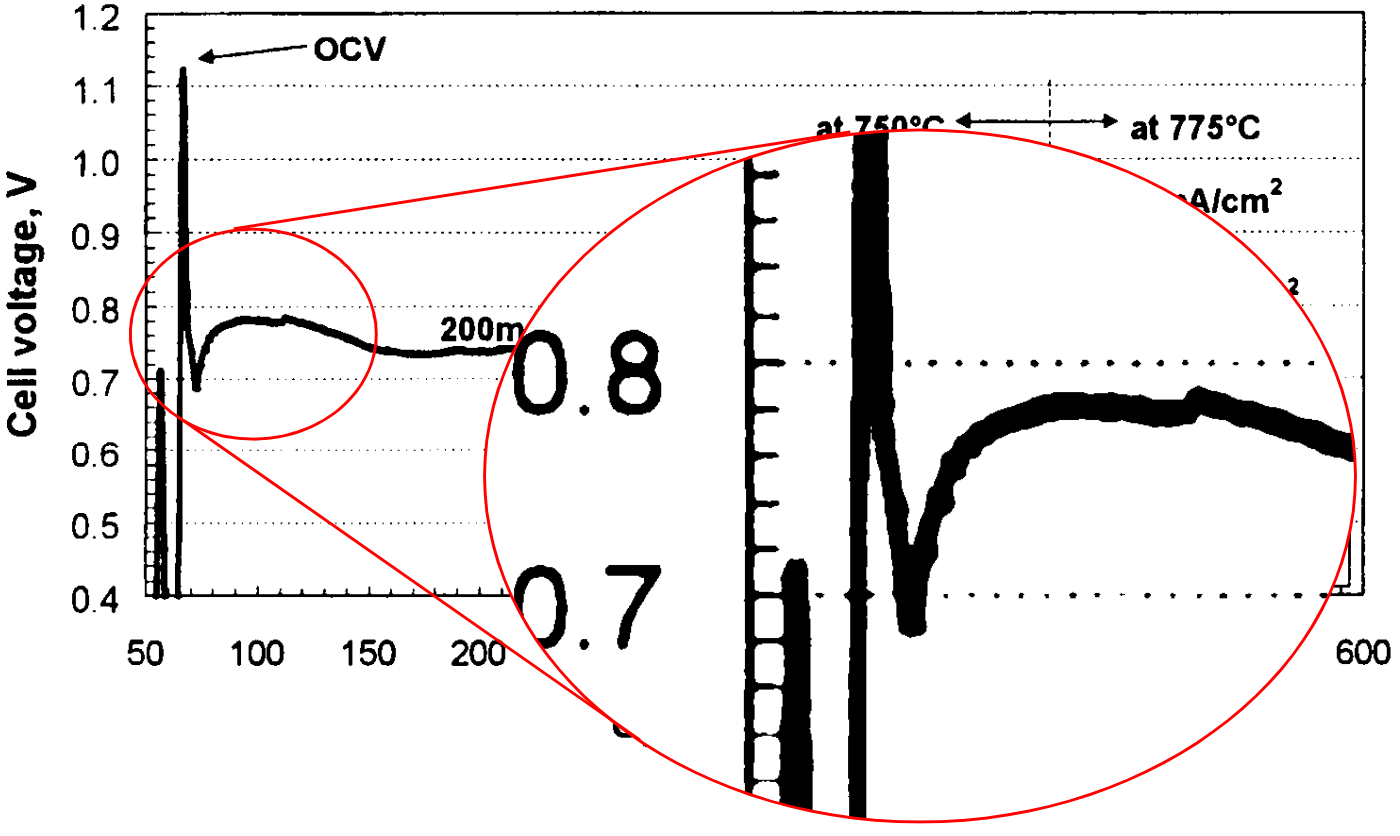

Figure 2. Cell performance at 750 and 775°C tested in alumina assembly

V_{start} : 0.68 V

V_{max} : 0.78 V

► V_{max}: Point of max. performance

► time to V_{max} : ≈ 50 hours

K. Föger et al., Demonstration of Anode Supported Cell Technology in kW Class Stack, Proc. 6th Int. Symp. on SOFC, Ed. S. Singhal und M. Dokiya, The Electrochemical Society, 95-100, PV 99-19, (1999)

SOFC: Formation and Long Term Test of a 1 kW Stack Mitsubishi Heavy Industries MHI (1999)

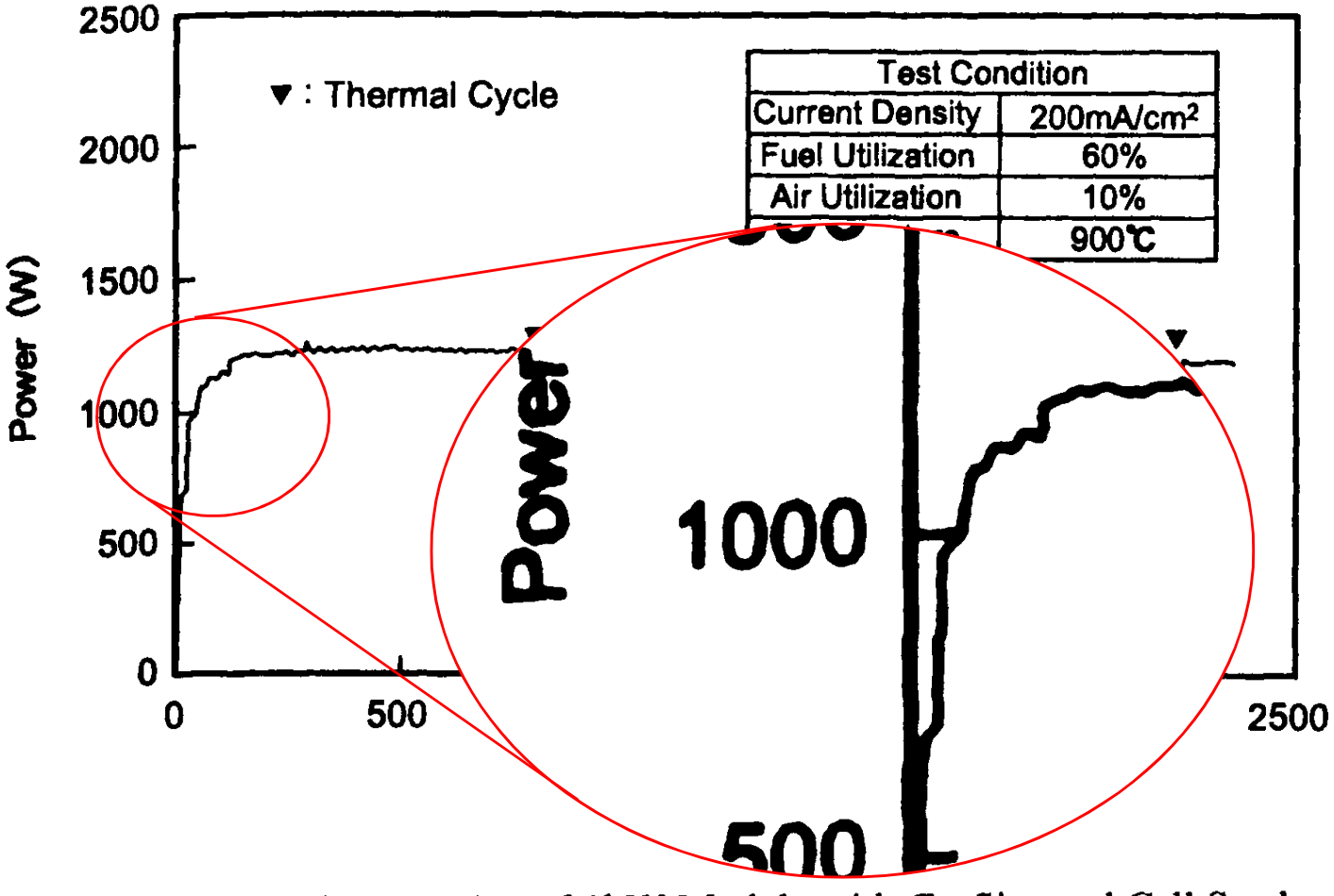

Fig. 12 Endurance Test of 1kW Module with Co-Sintered Cell Stack

P_{start} : 700 W

P_{max} : 1250 W

► P_{max}: Point of max. performance

► time to P_{max} :

≈ 300 hours

H. Mori et al., Pressurized 10 kW Class Module of SOFC, Proc. 6th Int. Symp. on SOFC, Ed. S. Singhal und M. Dokiya, - The Electrochemical Society, PV 99-19, 52-59, (1999)

Startup Behavior of SOFC Single Cells and Stacks
Formation and Degradation

max. performance	degradation
++	-
+	+
-	+

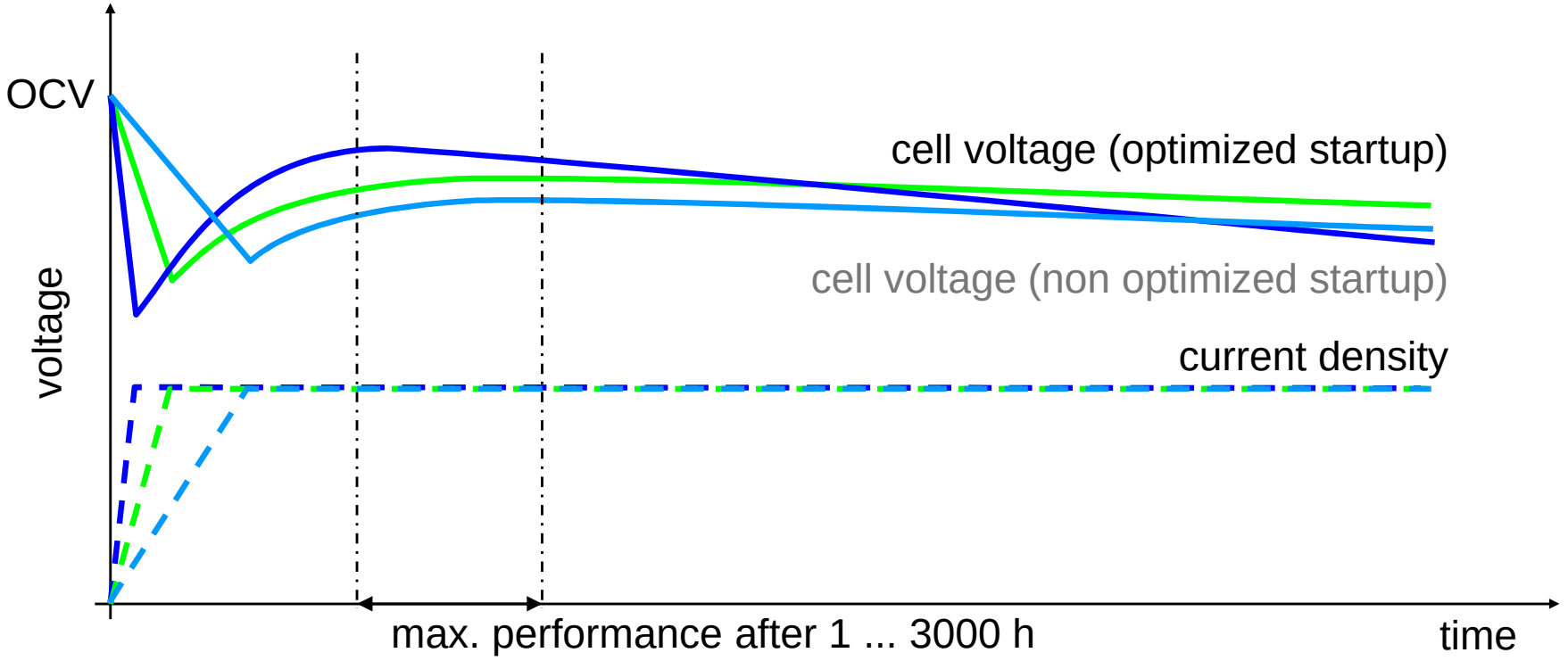

Cell Dynamics during Formation

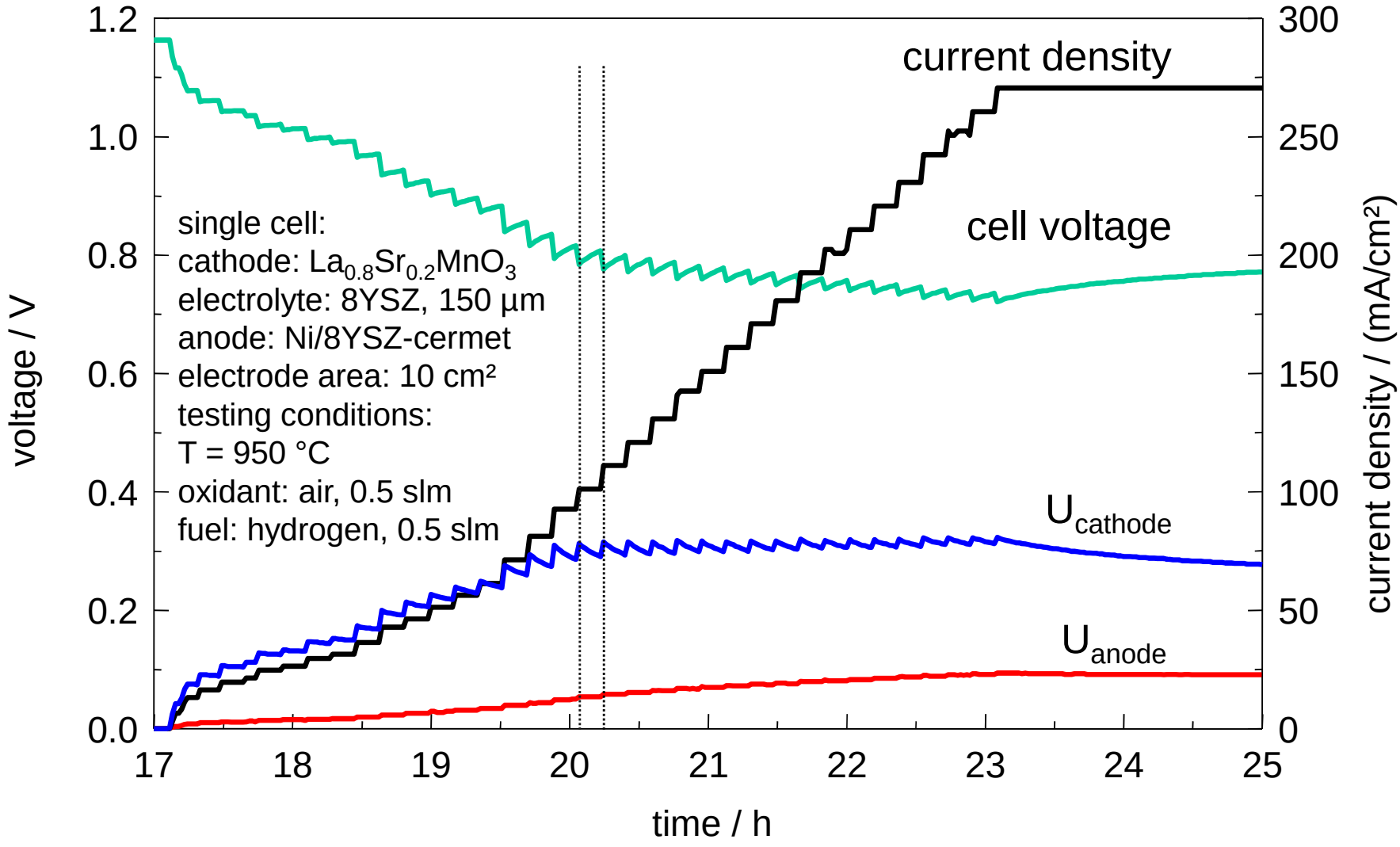

Cell Dynamics during Formation
Impedance Spectra of a single cell (Cathode: $La_{0.75}Sr_{0.2}MnO_3$)

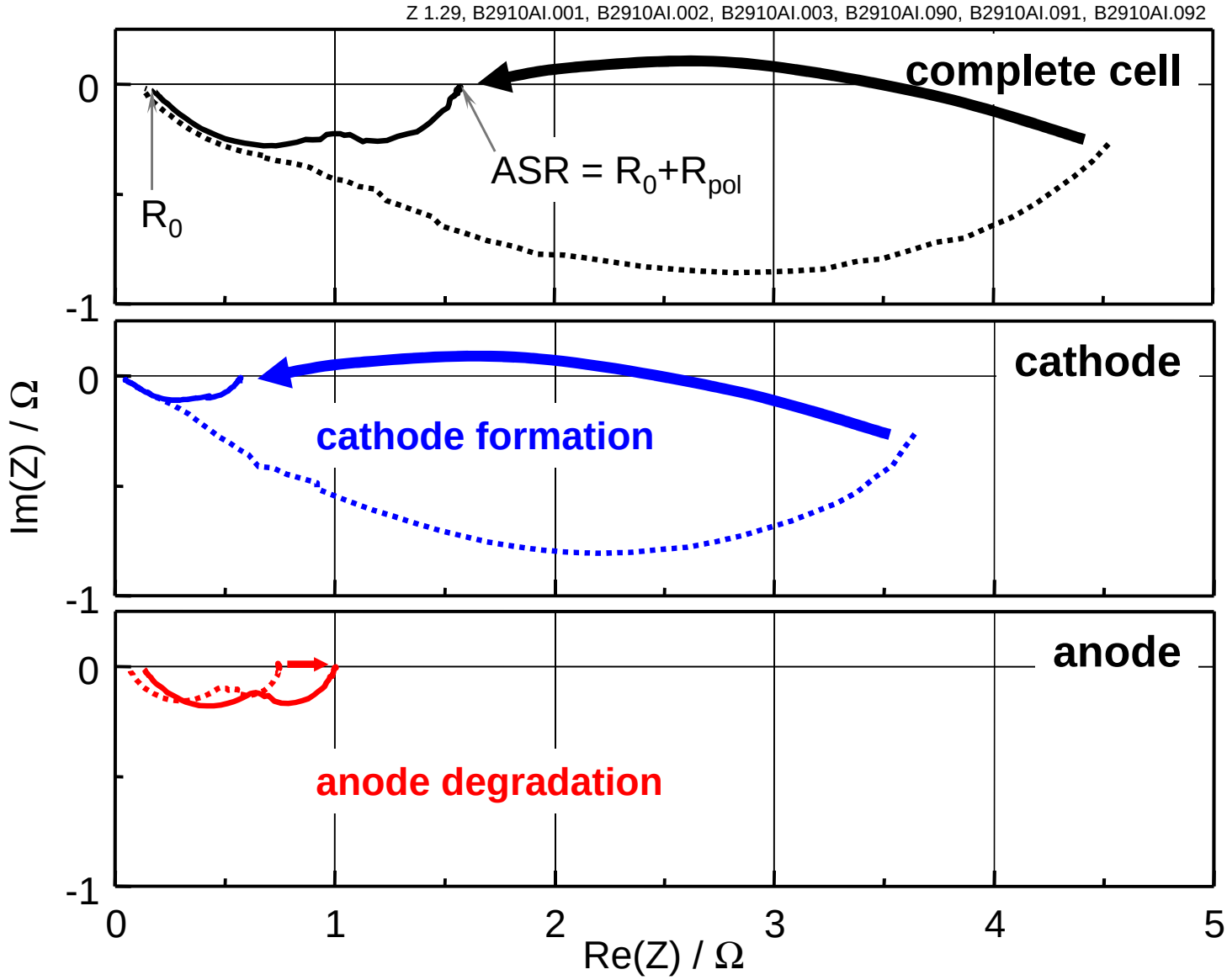

Start of formation

End of formation

cell 1.29
cathode: $La_{0.75}Sr_{0.2}MnO_3$
electrolyte: 8YSZ
anode: Ni/8YSZ - cermet
electrode area: 1 cm²
oxidant: air, 0.25 slm
fuel: hydrogen, 0.25 slm
temperature: 950 °C

impedance spectroscopy:
amplitude: 6 mA/cm²
bias: 6 mA/cm²
frequency: 0.1 Hz ... 300 kHz

Formierung von SOFC-Kathoden
Veränderung der Mikrostuktur der LSM-Kathode

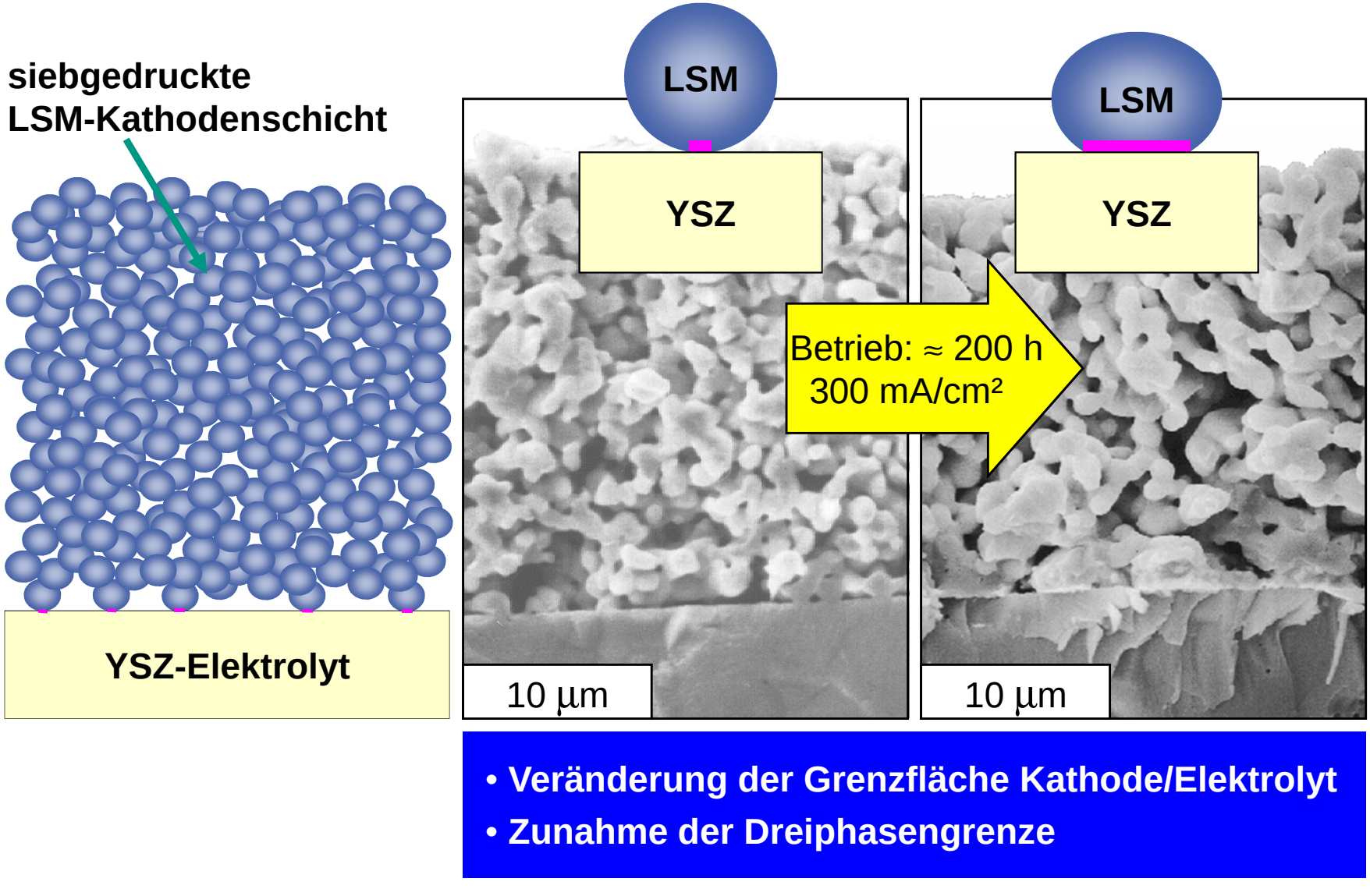

- **Veränderung der Grenzfläche Kathode/Elektrolyt**
- **Zunahme der Dreiphasengrenze**

REM: Grenzfläche Kathode-Elektrolyt vor und nach Aktivierung

unbelastete MEA

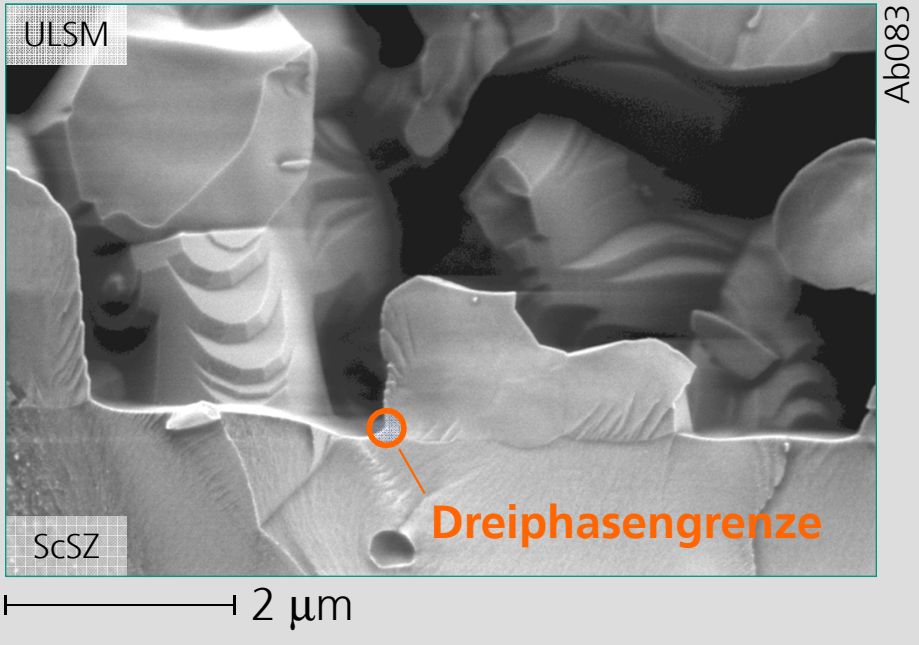

nach Aktivierung

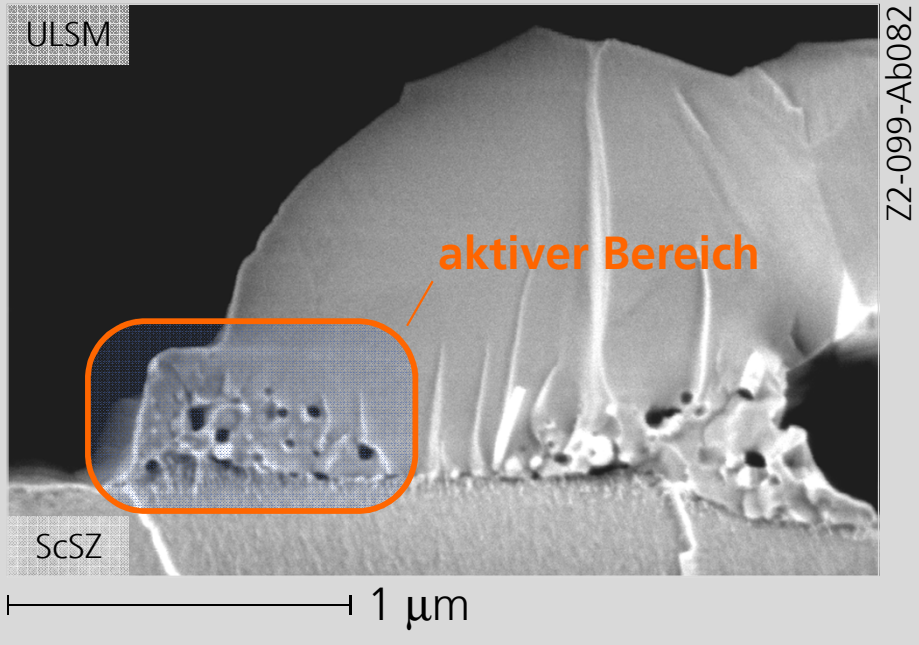

- Bildung eines porösen Bereichs im ULSM-Korn nahe der Grenzfläche unter Belastung
- Reaktionsraum vergrößert ⇨ höhere elektrochemische Leistungsfähigkeit der Kathode

Formierung von SOFC-Kathoden
Veränderung der Grenzfläche Kathode/Elektrolyt

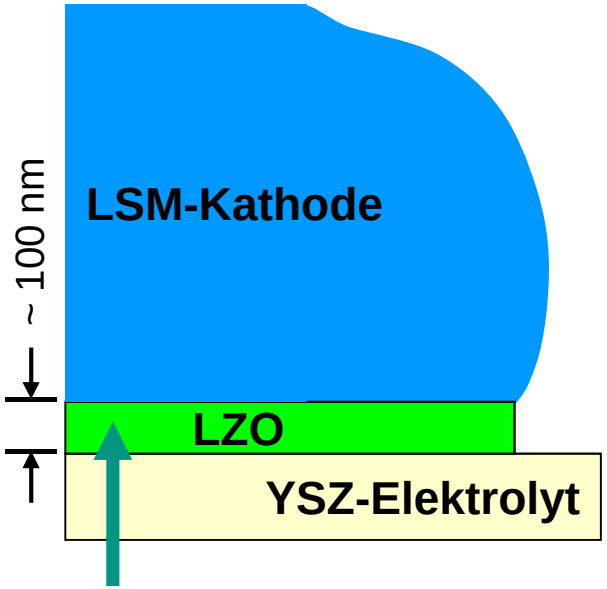

Lanthanzirkonat- (LZO-) Zwischenschicht

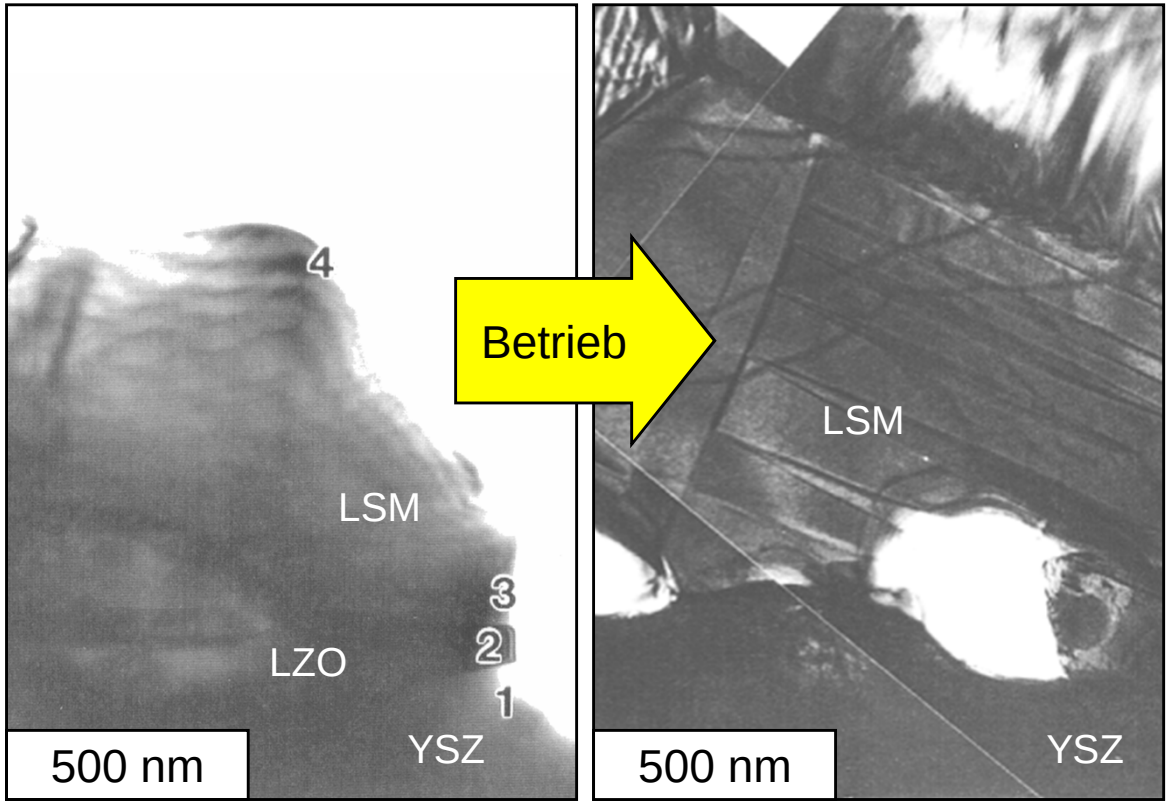

- **Abbau der LZO-Zwischenschicht**
- **Ausbildung von Mikroporen**

Elektrolyt:
Verlust ionischer Leitfähigkeit

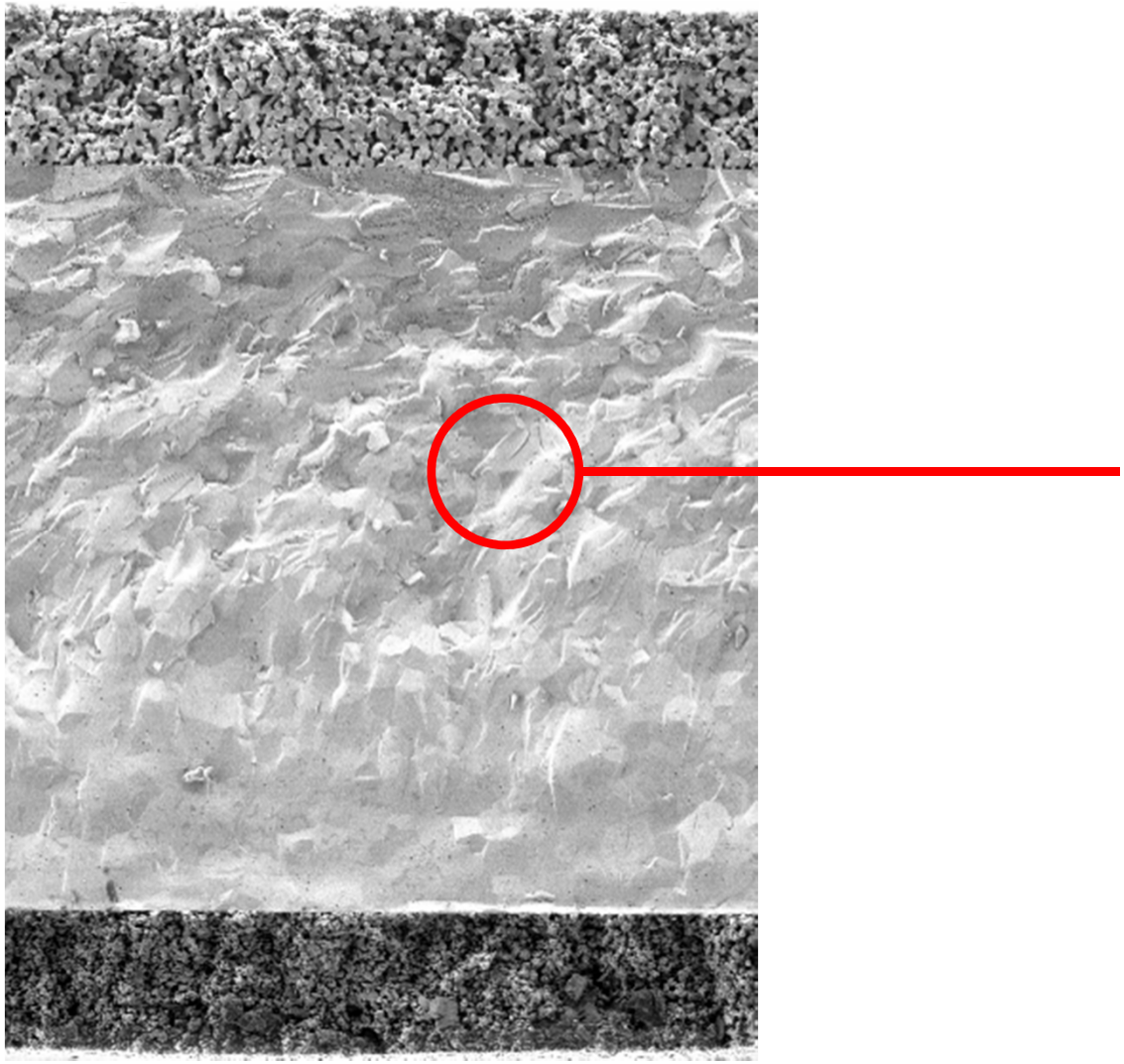

Yttria doped Zirconia (YSZ) Phase Diagram

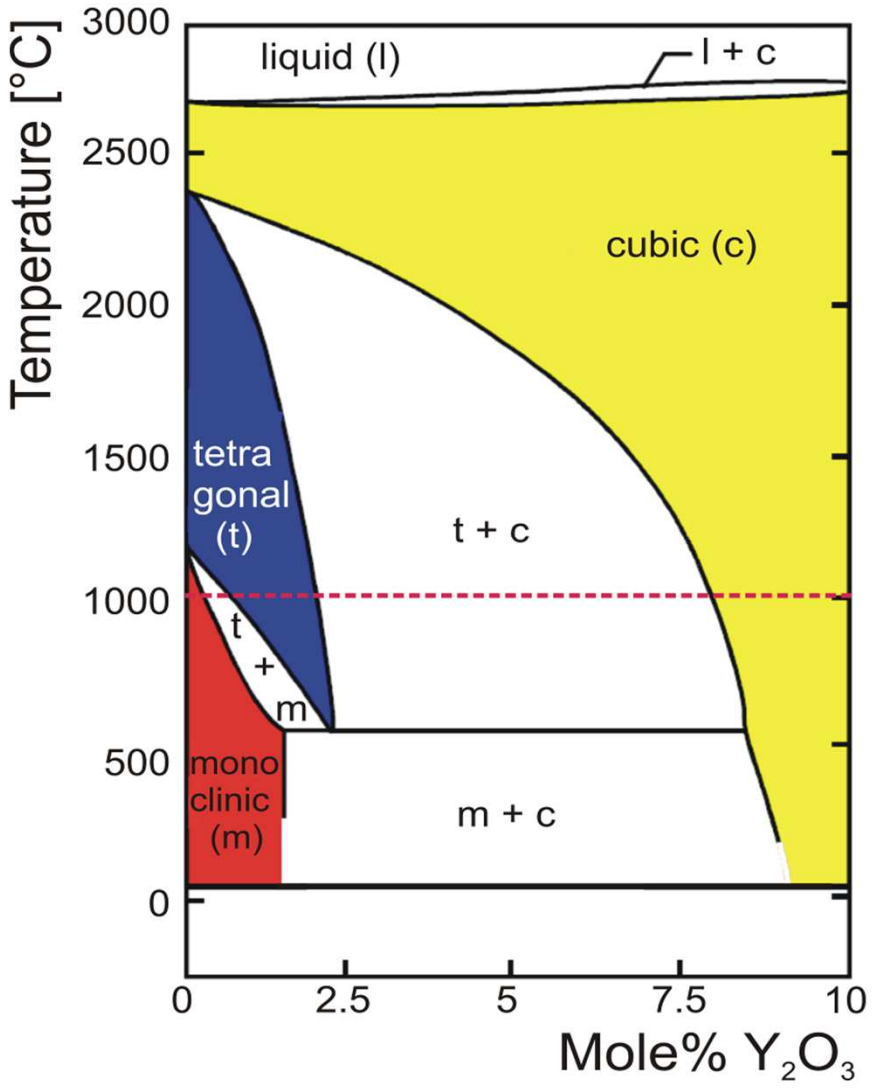

FSZ
Fully Stabilized Zirconia
cubic
≥ 8 mol% Y_2O_3

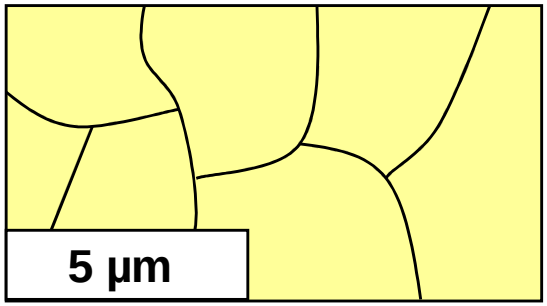

TZP
Tetragonal Zirconia Polycrystal
tetragonal
≤ 3 mol% Y_2O_3

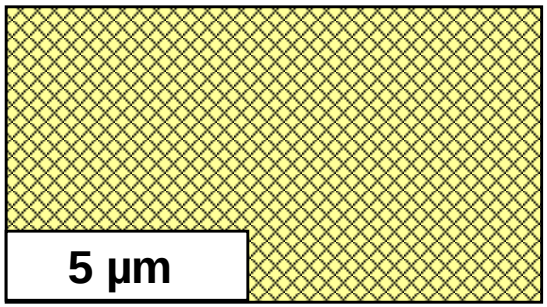

Electrical Conductivity of Fluorites $ZrO_2 – Me_2O_3$
Impact of various dopants on the conductivity of ZrO_2

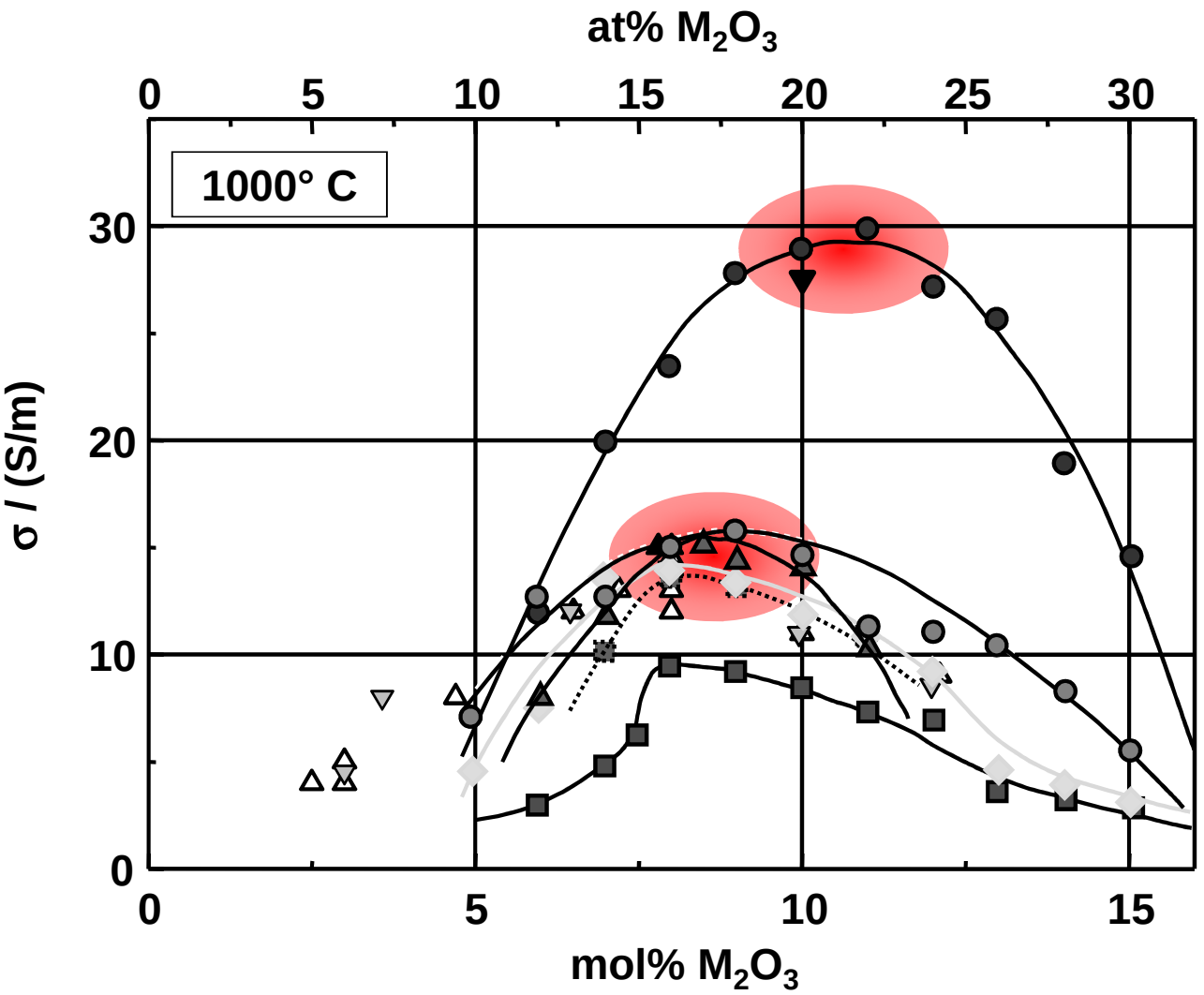

- Y [1]
- Y [2]
- Y [3]
- Gd [1]
- Yb [1]
- Er [1]
- Dy [1]
- Sc [1]
- Sc [4]

[1] O. Yamamoto, Electrochimica Acta 45, p. 2423 (2000)

[2] R. Männer, Electroceramics and Ceramics for Special Applications, Vol. 3, DKG (1992)

[3] Siemens, unpublished data

[4] D. Herbstritt, The Electrochemical Society, PV 2001-16, p. 349, (2001)

Long term stability of of ZrO_2 – Me_2O_3 Oxide Ion Conductors
FSZ: 8YSZ

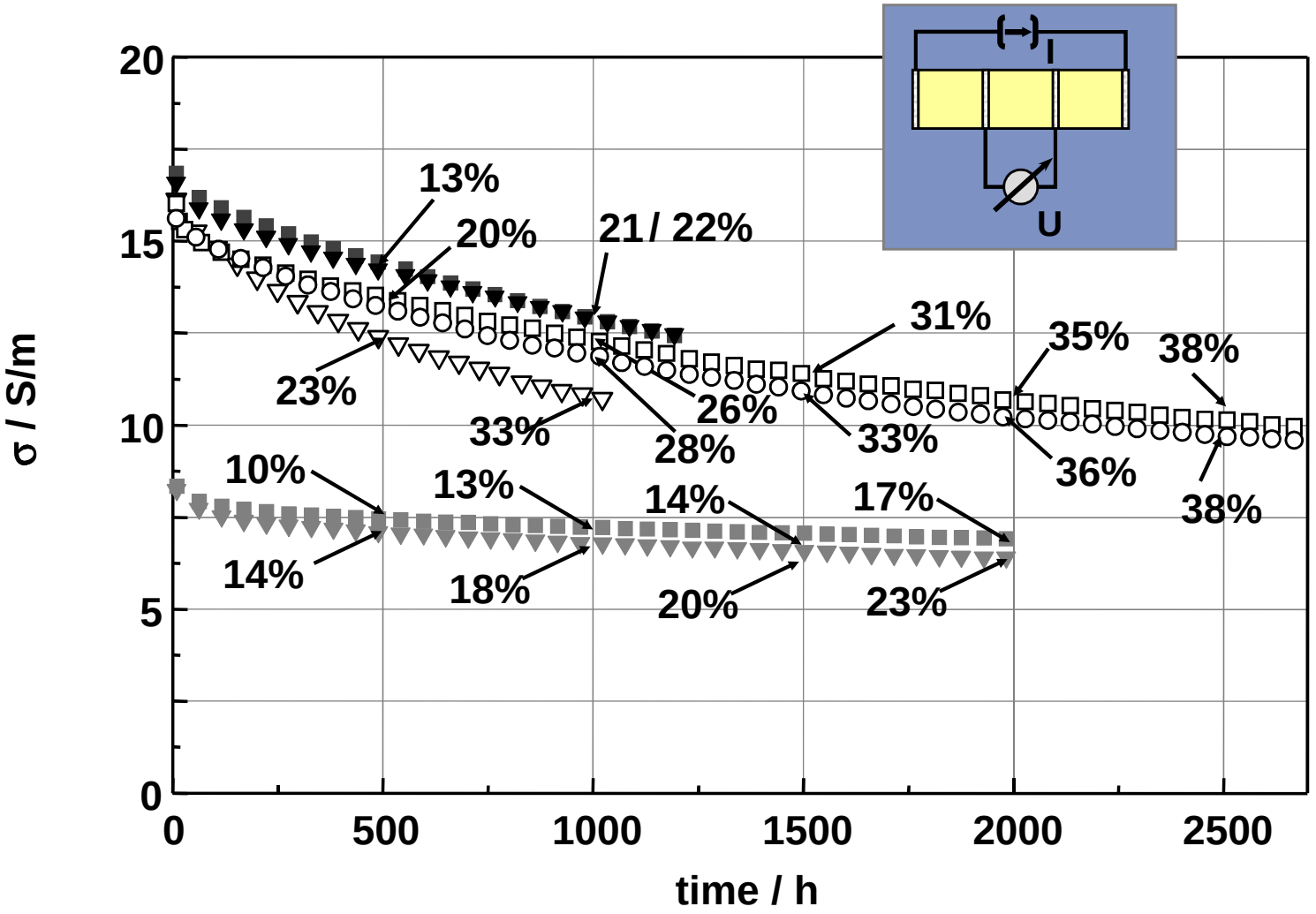

T_{op}=956°C, 170mA/cm²

○ **8YSZ, T_{sint}=1550°C**

□ **8YSZ, RCS @ 1500°C**

▽ **8YSZ, RCS @ 1350°C**

T_{op}=956°C, 600mA/cm²

■ **8YSZ, RCS @ 1500°C**

▼ **8YSZ, RCS @ 1350°C**

T_{op}=861°C, 120mA/cm²

■ **8YSZ, RCS @ 1500°C**

▼ **8YSZ, RCS @ 1350°C**

RCS:
rate controlled sintering
constant shrinkage

Long term stability of of ZrO_2 – Me_2O_3 Oxide Ion Conductors TZP: 3YSZ and 4ScSZ

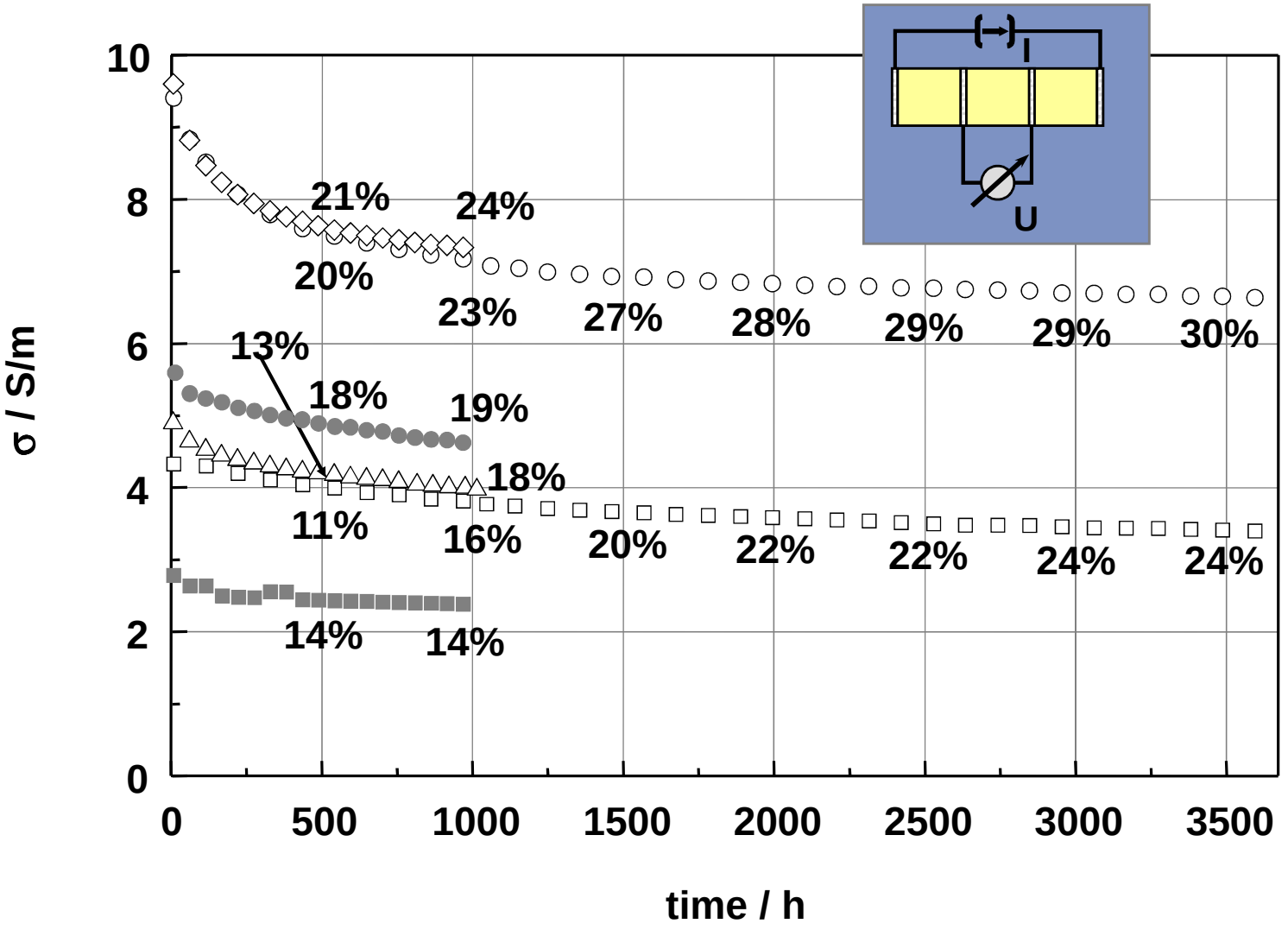

T_{op}=956°C, 170mA/cm²

- 3YSZ, T_{sint}=1430°C
- 3YSZ, T_{sint}=1300°C
- 4ScSZ, T_{sint}=1350°C
- 4ScSZ, T_{sint}=1300°C

T_{op}=861°C, 120mA/cm²

- 3YSZ, T_{sint}=1430°C
- 4ScSZ, T_{sint}=1350°C

Long term stability of of ZrO_2 – Me_2O_3 Oxide Ion Conductors FSZ: 10YSZ and 10ScSZ

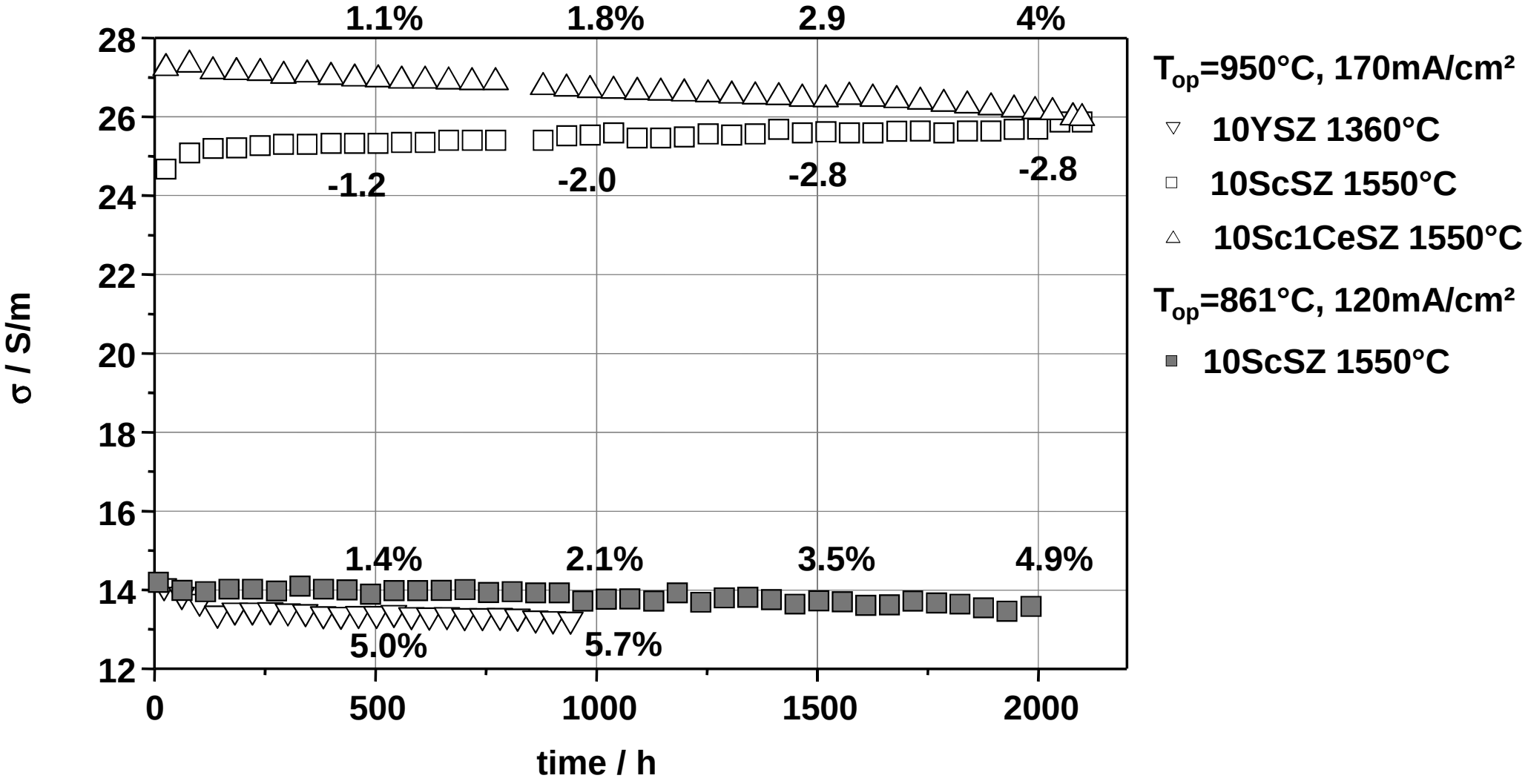

T_{op}=950°C, 170mA/cm²

▽ 10YSZ 1360°C

□ 10ScSZ 1550°C

△ 10Sc1CeSZ 1550°C

T_{op}=861°C, 120mA/cm²

■ 10ScSZ 1550°C

Long Term Stability of Electrolyte supported Single Cells with 8YSZ and 10ScSZ Electrolyte Substrate

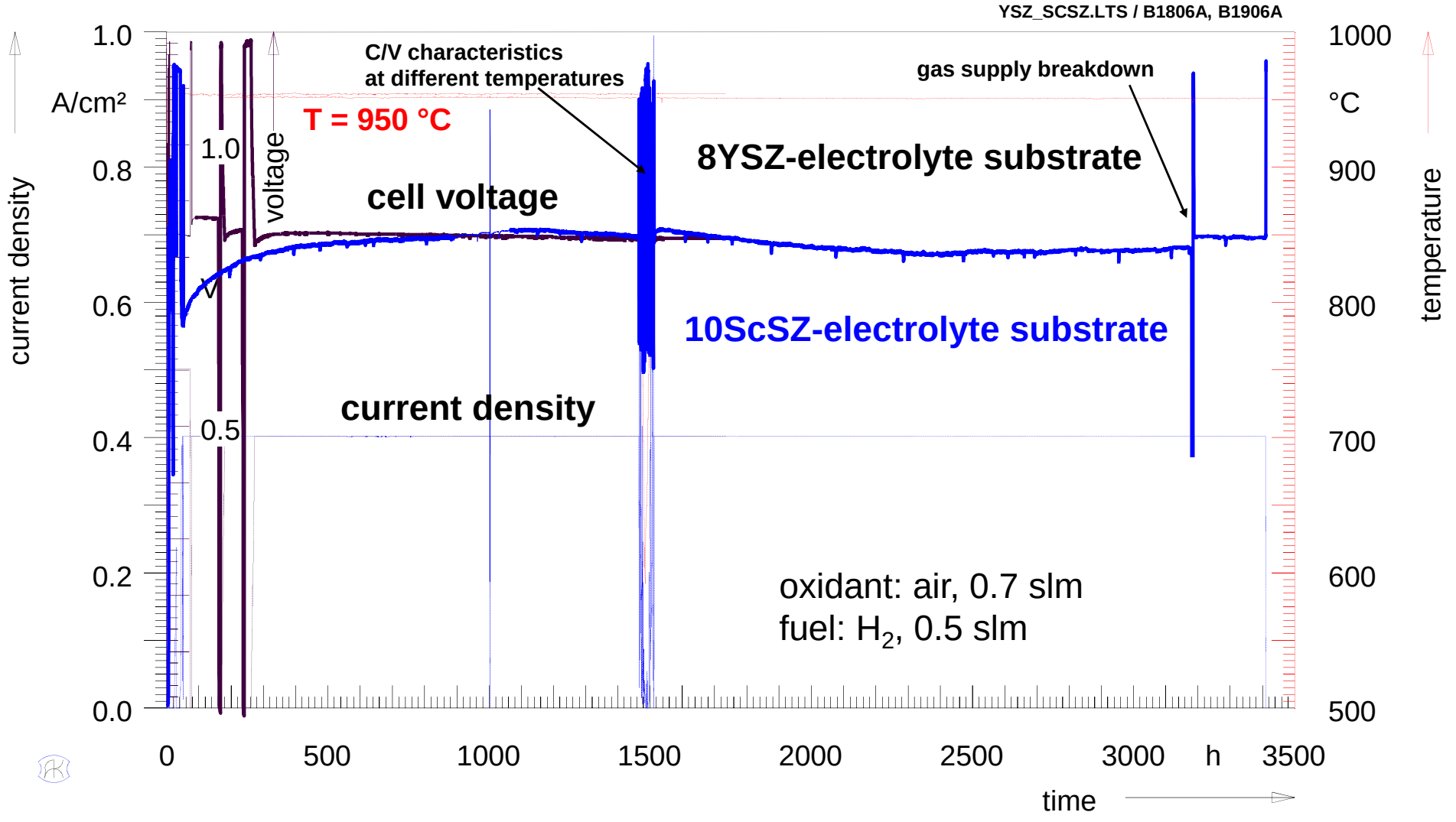

Electrolyte Degradation ( )
Long term stability: 10ScSZ ( ) vs. 8YSZ ( ) at 950°C

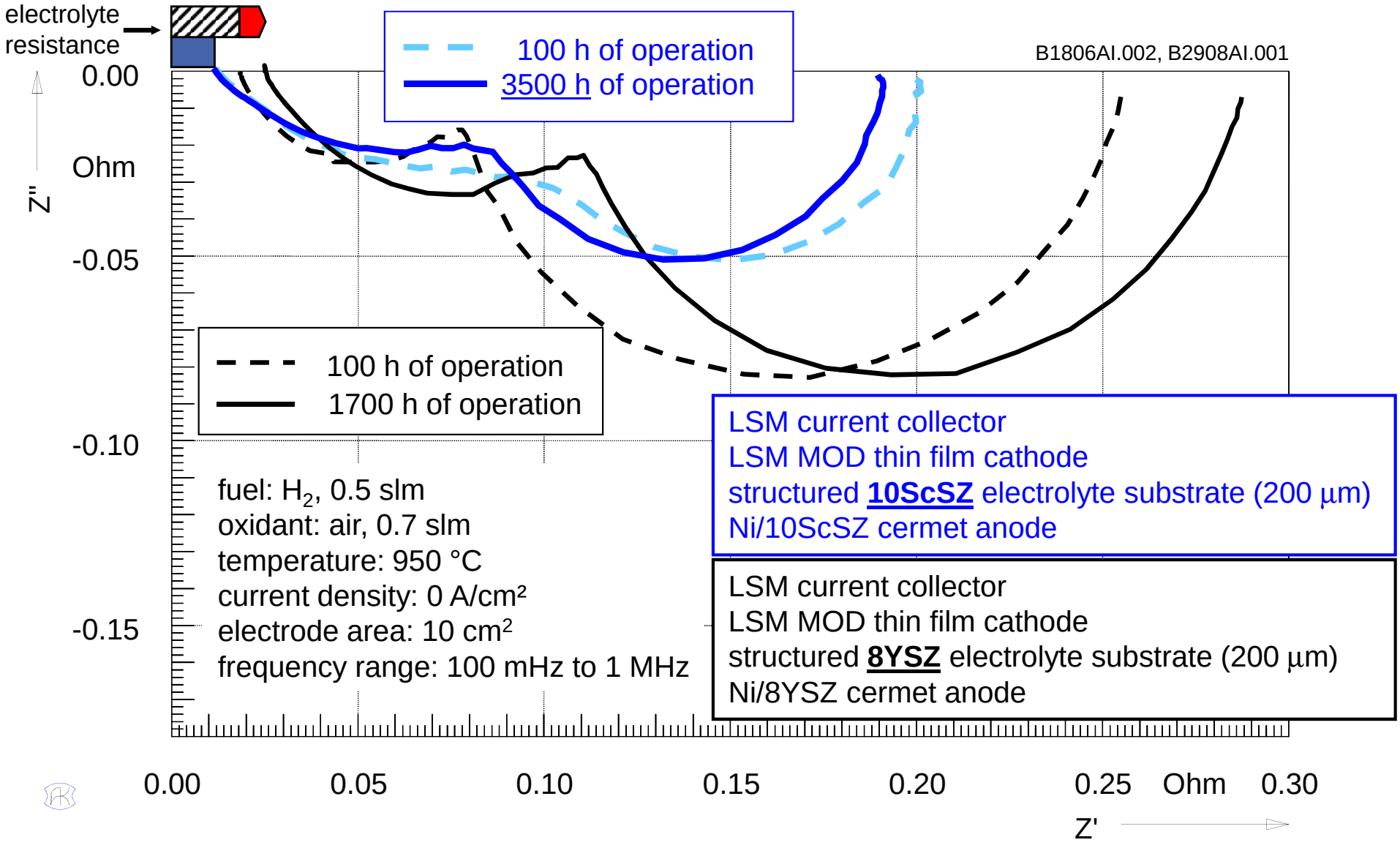

Electron diffraction: Tetragonal Phase

[110], [111], [112], [013], [123]

- Three variants of tetragonal phase:
  c-axis along all cubic <100>-axes
- Double diffraction in thicker sample regions

→ Clear identification of tetragonal phase
(no superstructures!)

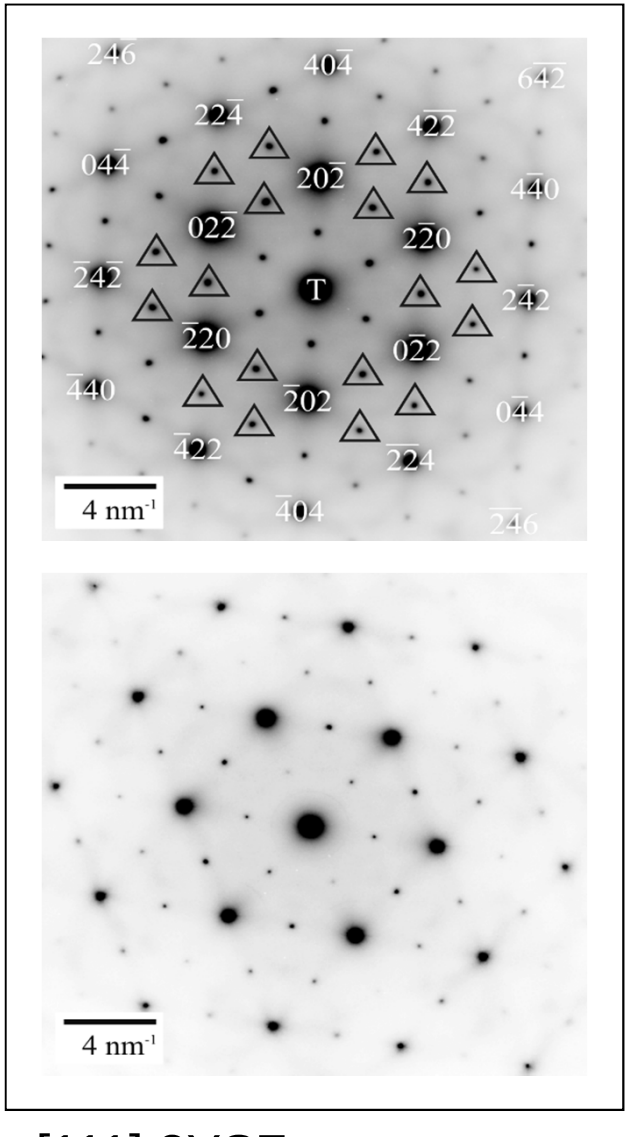

[111] 8YSZ

Electron diffraction

- Exists in 8YSZ and 10YSZ, not in 16YSZ
- Decreasing volume fraction with increasing doping concentration

→ Dark field images with tetragonal intensity

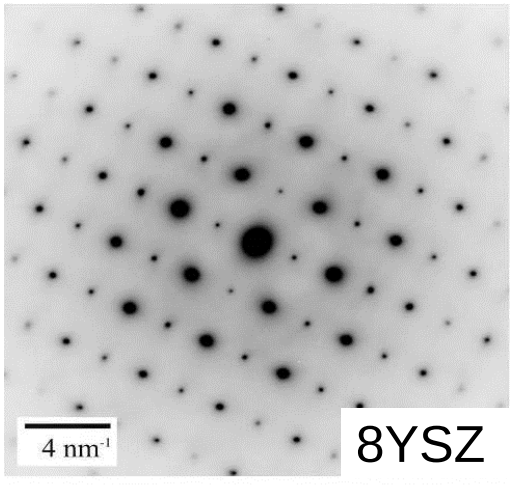

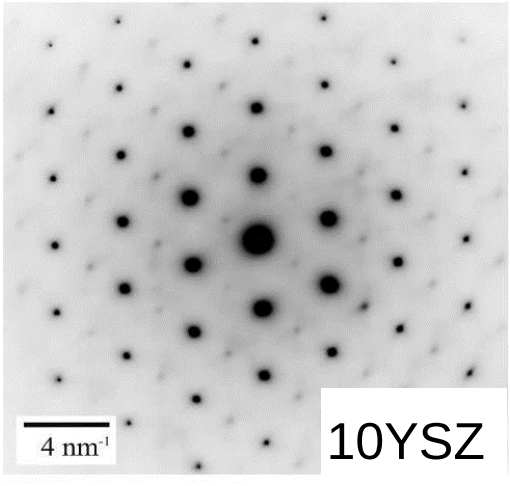

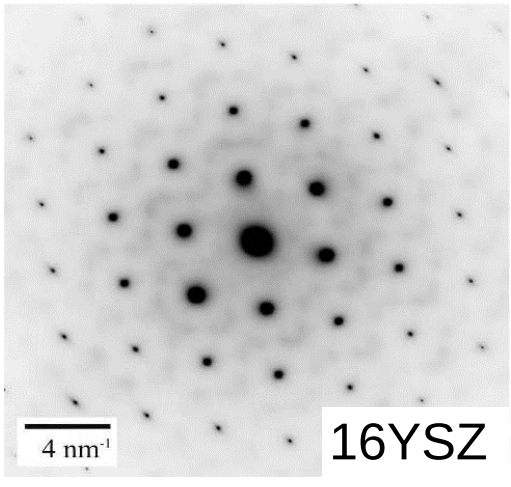

Anode:
Agglomeration der Nickel-Partikel

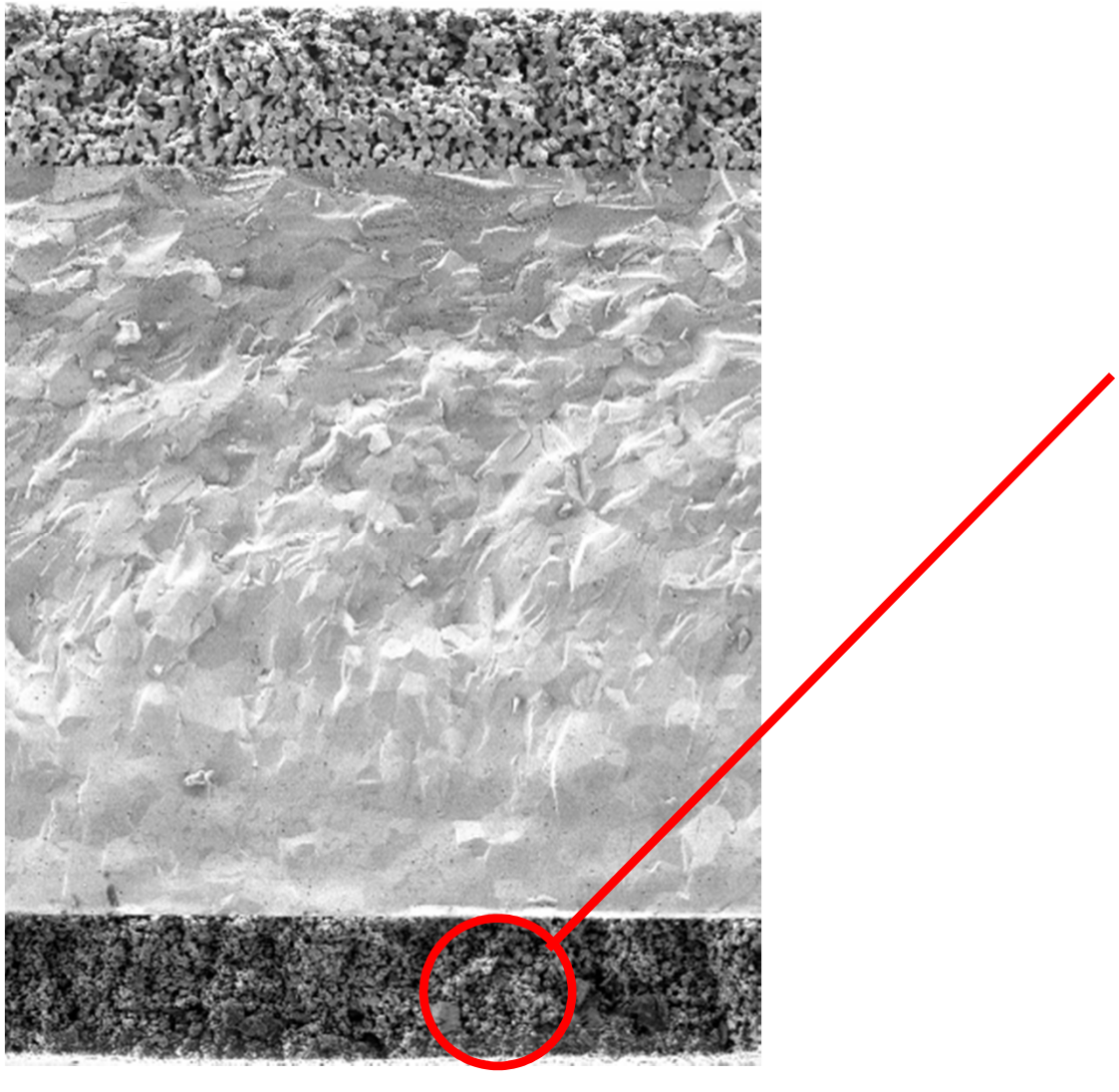

Anode Degradation
Stack position and fuel utilization

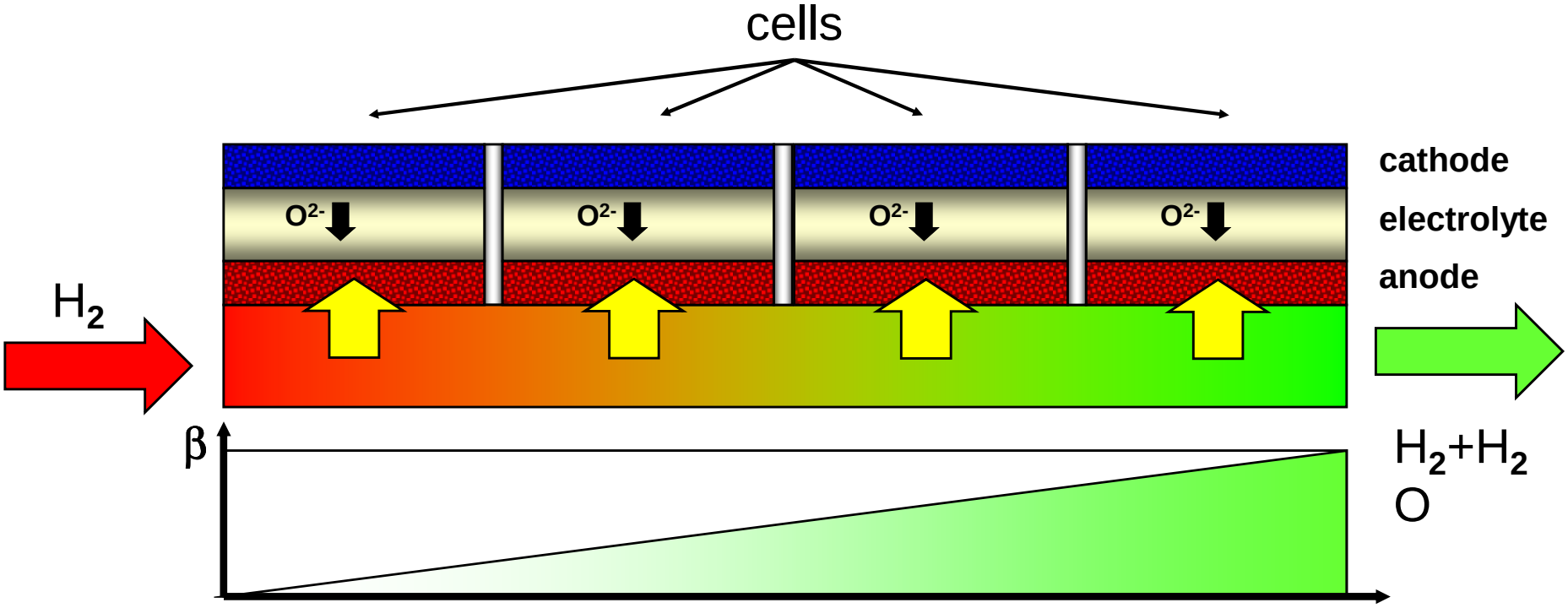

position of the cell in the layer of a stack

fuel utilization: $\beta = \frac{p(H_2O)}{p(H_2O)+p(H_2)}$

Anode Degradation
Influence of current density and fuel utilization

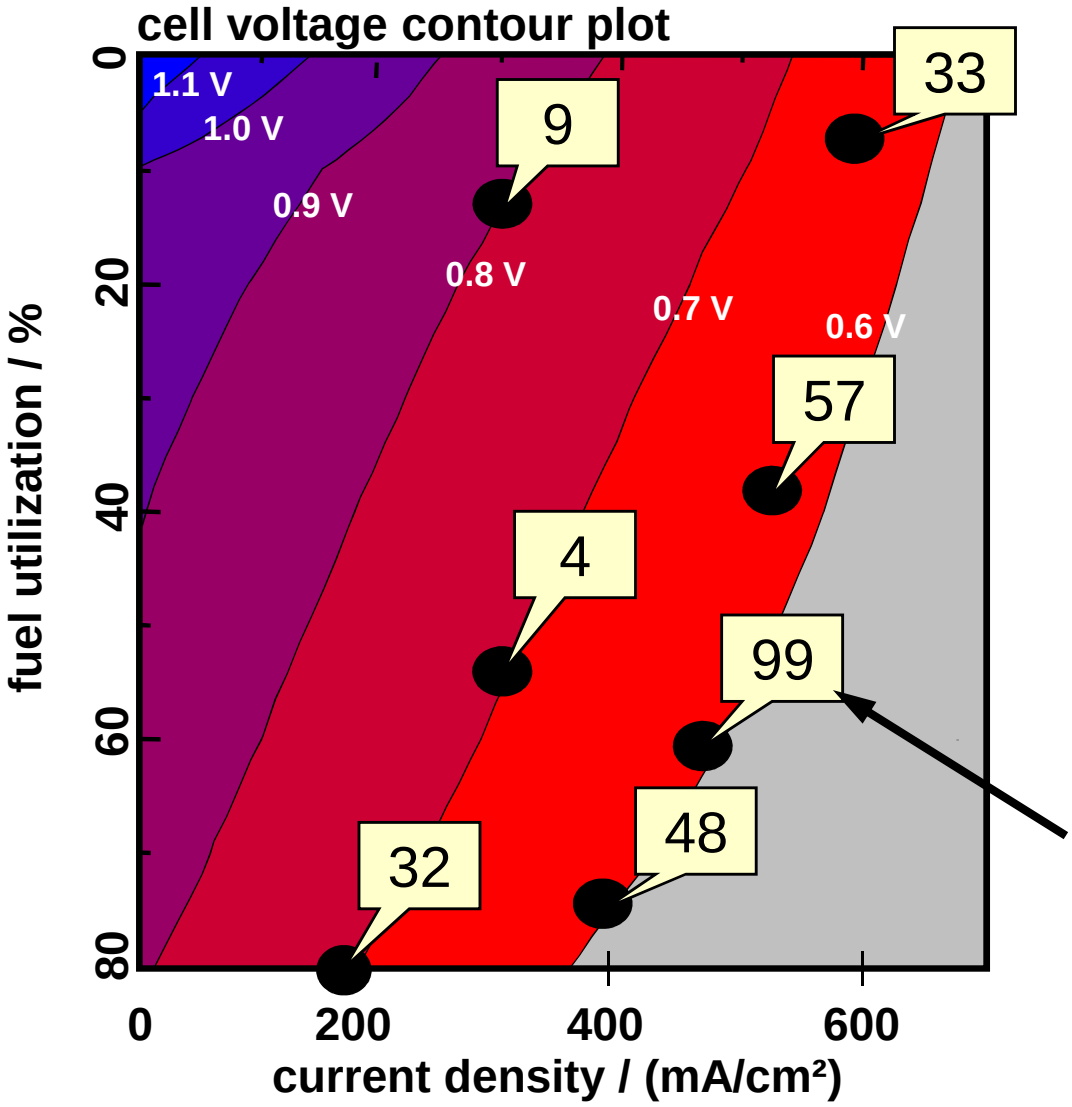

Performance plot

Long term measurements
Operation time: 700 ... 1000 h
Temperature : 950 °C
Oxidant : air

Aim: <1 mV/1000h

Degradation rates in mV/1000h

Anode Degradation
Ni-Agglomeration

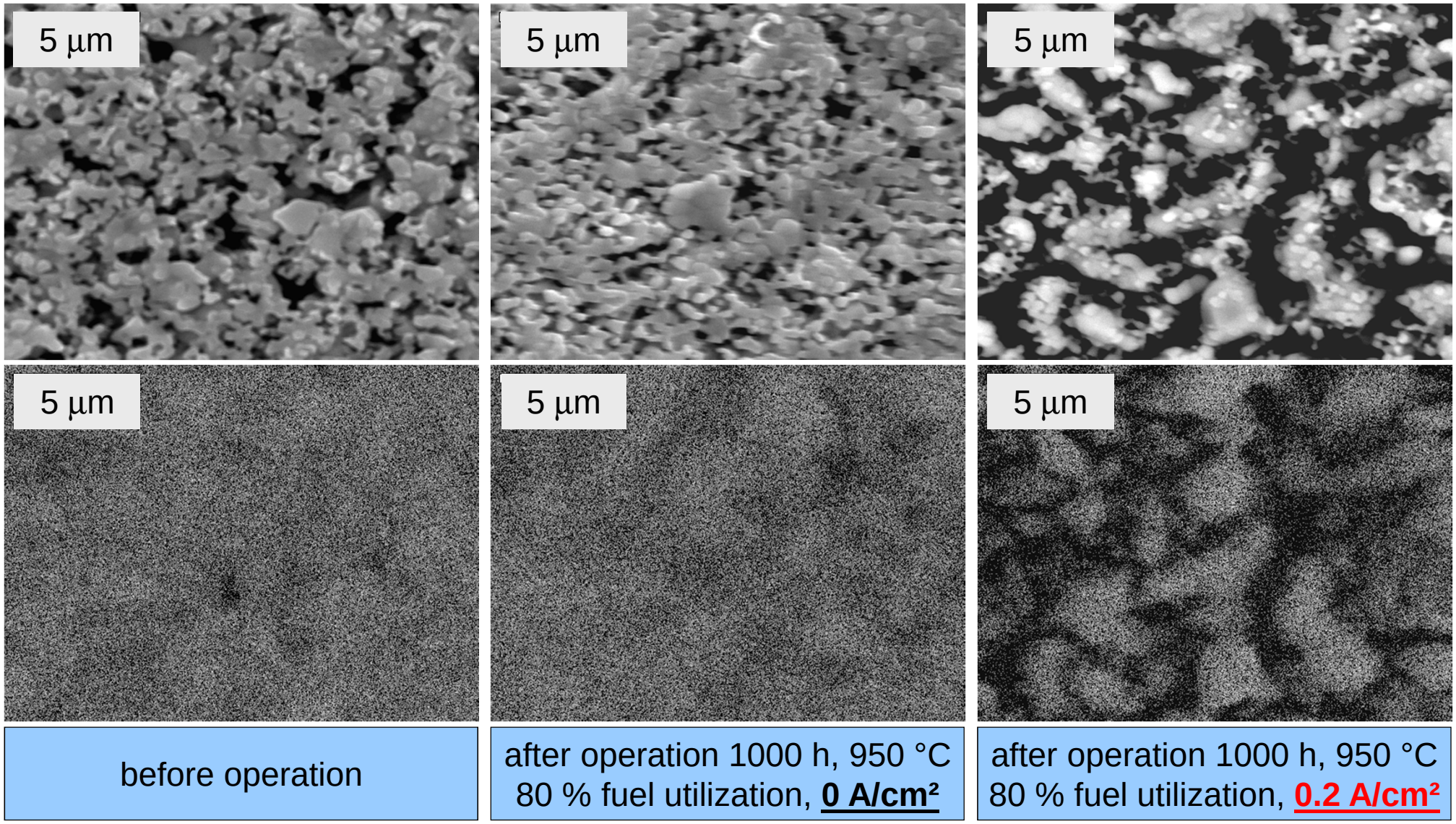

before operation	after operation 1000 h, 950 °C 80 % fuel utilization, **0 A/cm²**	after operation 1000 h, 950 °C 80 % fuel utilization, **0.2 A/cm²**

Anode:
Alterung unter Redox-Zyklen

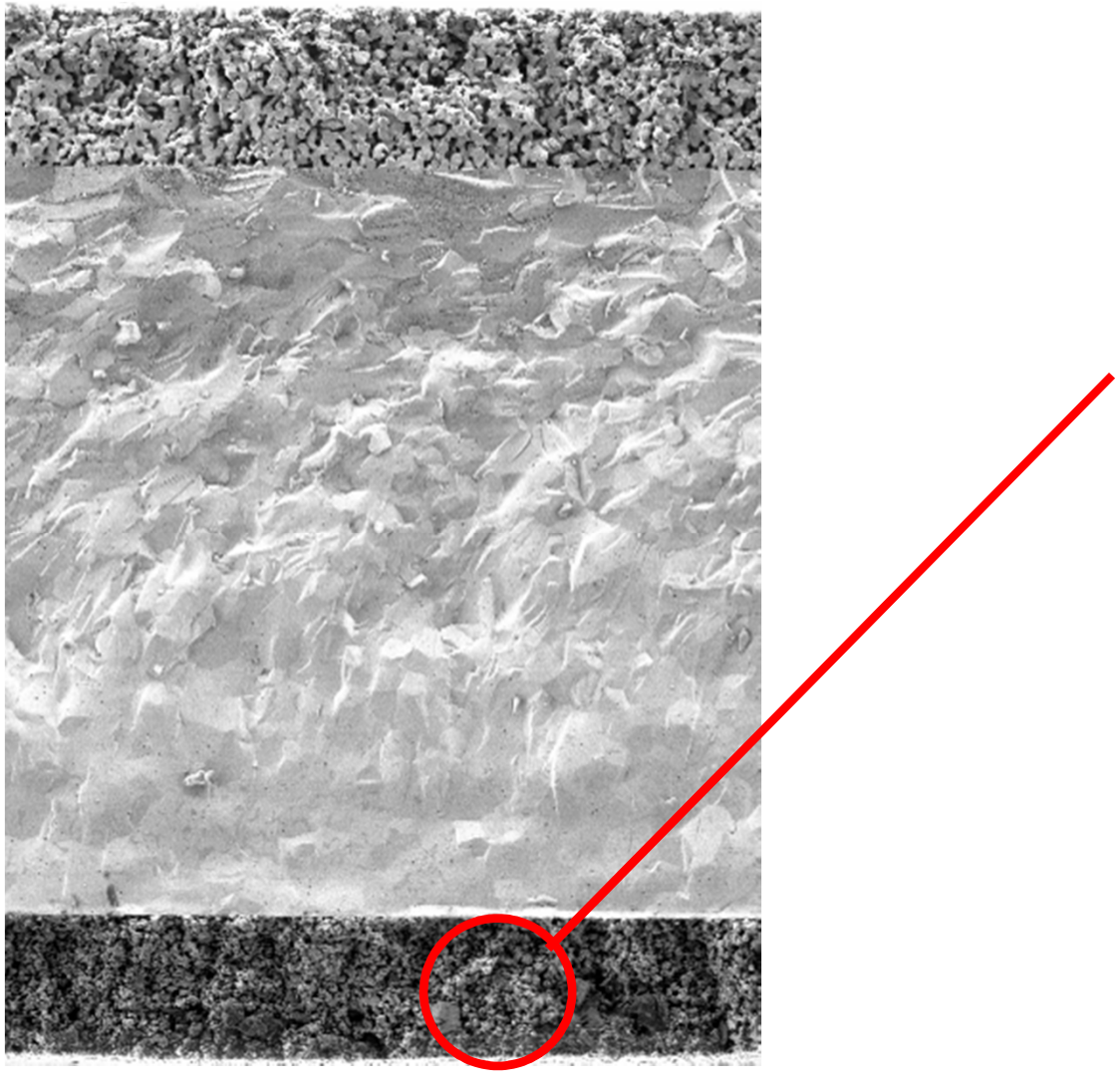

Anode
Redox-Stability

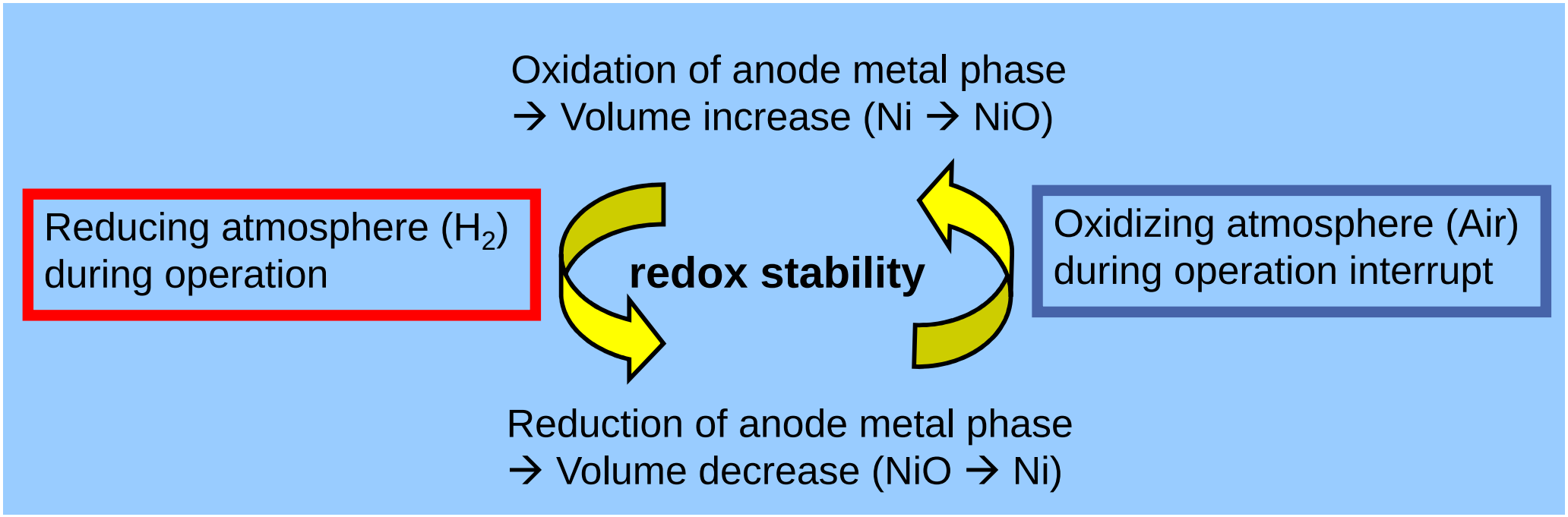

Extrinsic Degradation
Cracking of an Anode Supported Electrolyte after Redox-Cycling

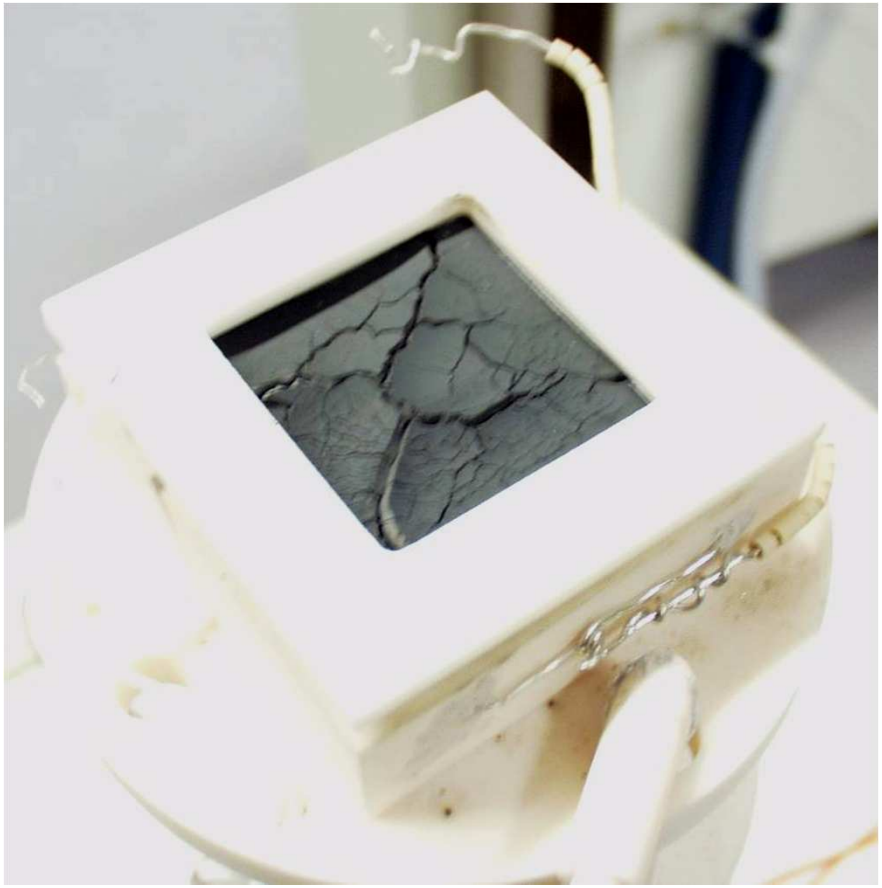

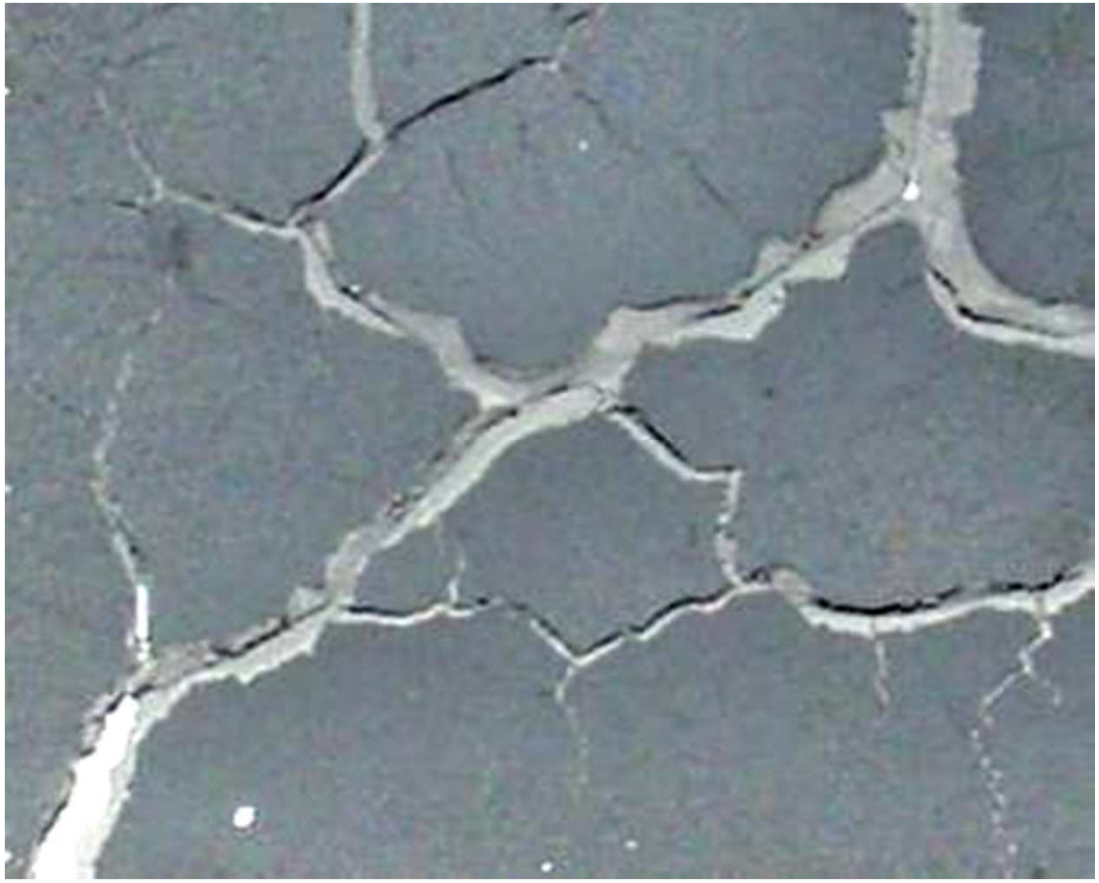

Impact of Redox Cycle on Length Change of Ni/YSZ Bulks: Different Sintering Temperatures

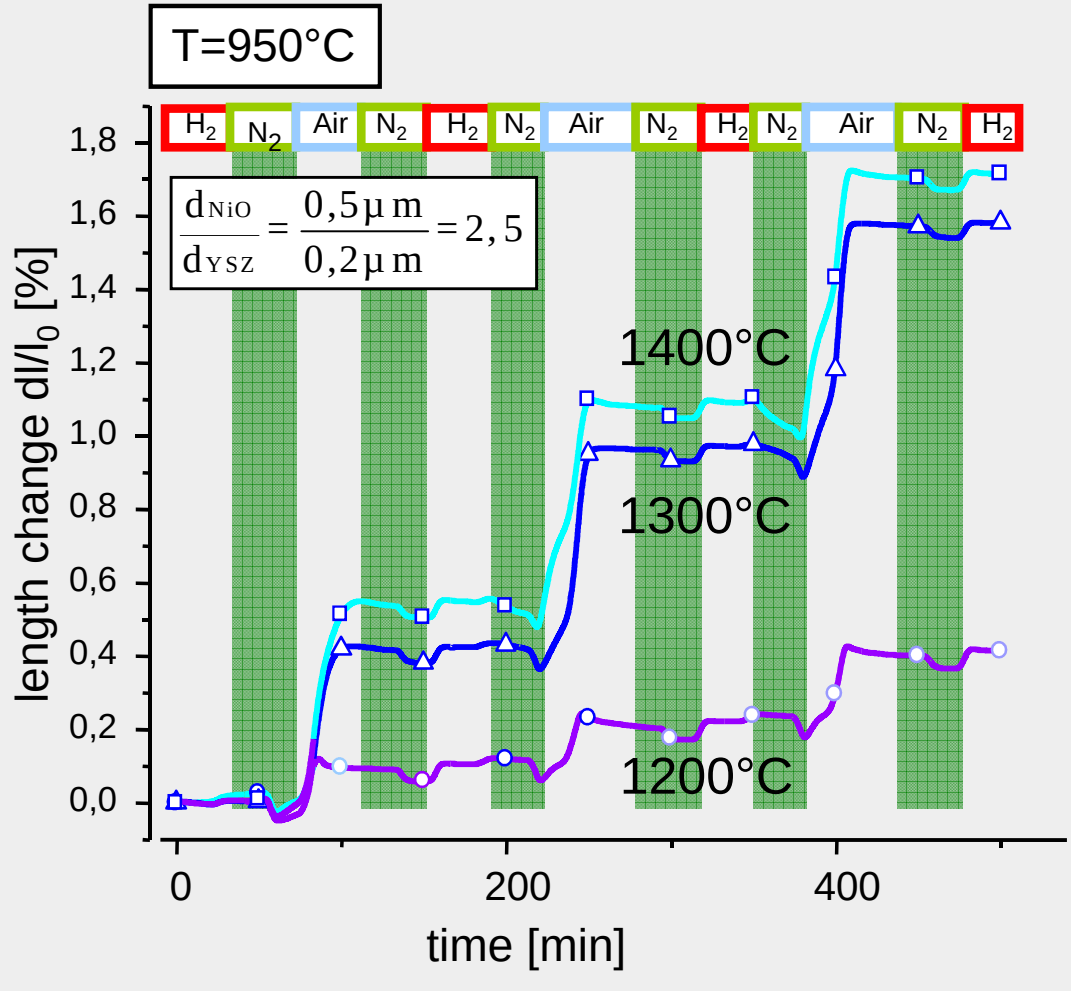

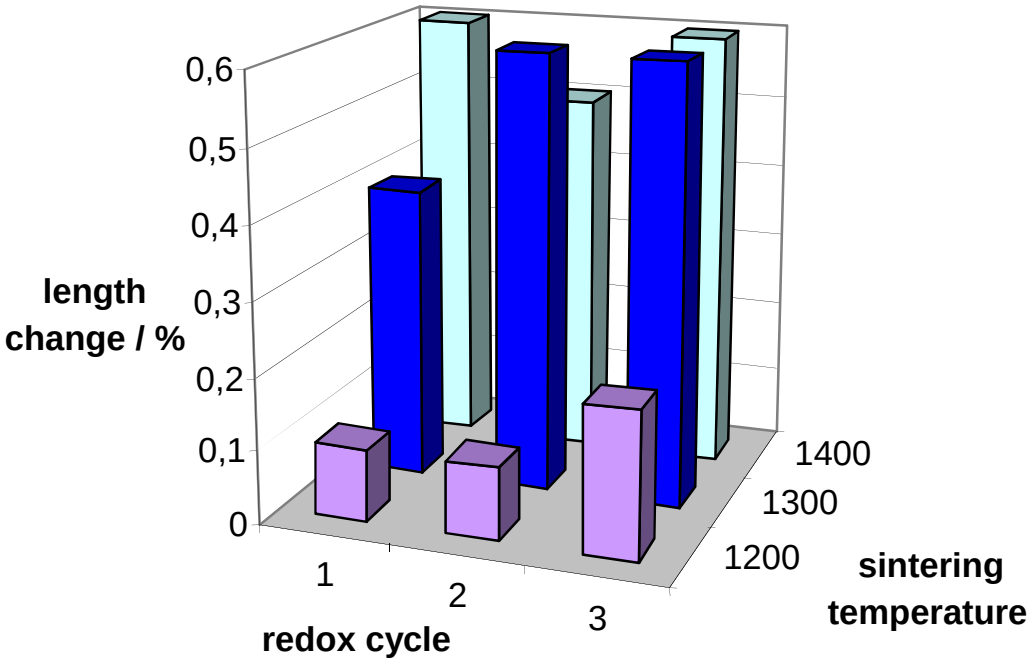

➢ minimum length change at lowest sintering temperature of 1200 °C

Impact of Redox Cycles on Microstructure of Ni/YSZ Bulks Different Sintering Temperatures

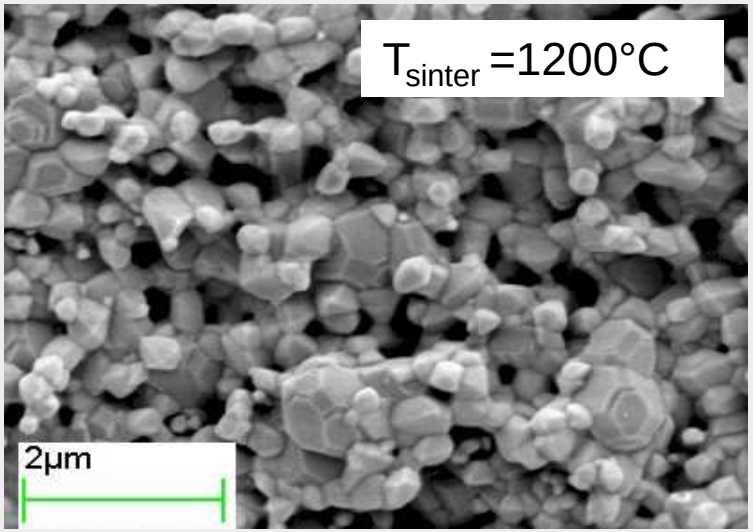

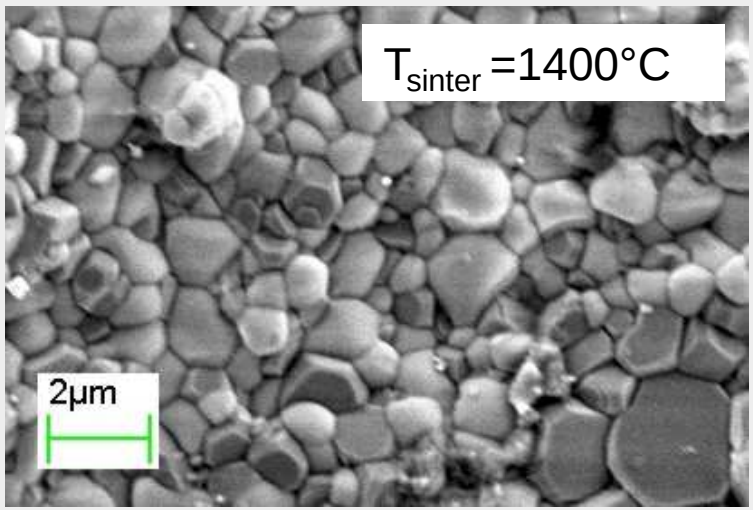

d_{50}: NiO=0,5µm
d_{50}: YSZ=0,2µm

length change
dl/l_0 = 0,4%

3 redox cycles

length change
dl/l_0 = 1,7%

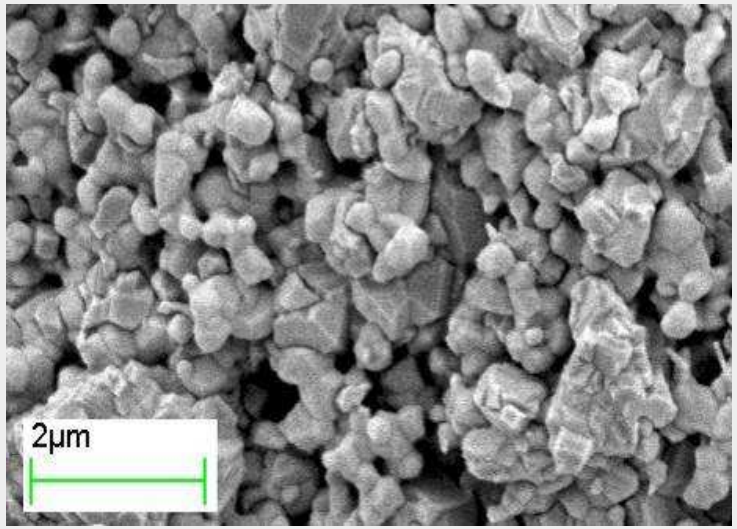

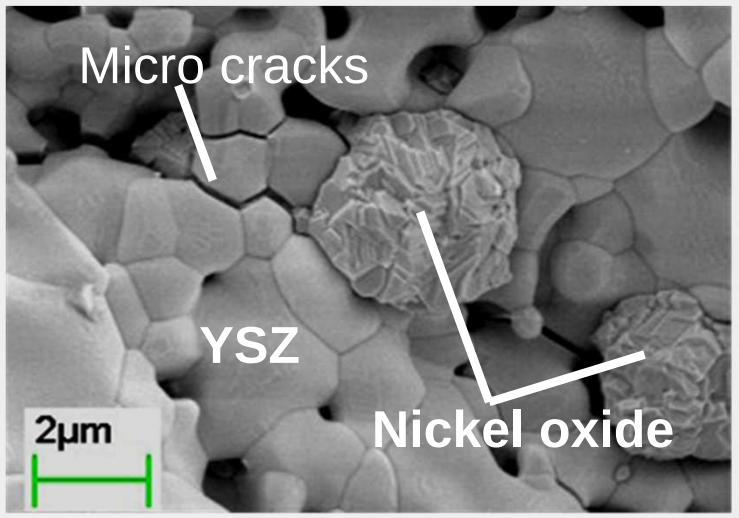

Degradation Tests for SOFC
Redox Stability (100 Redox-Cycles in 35 h)

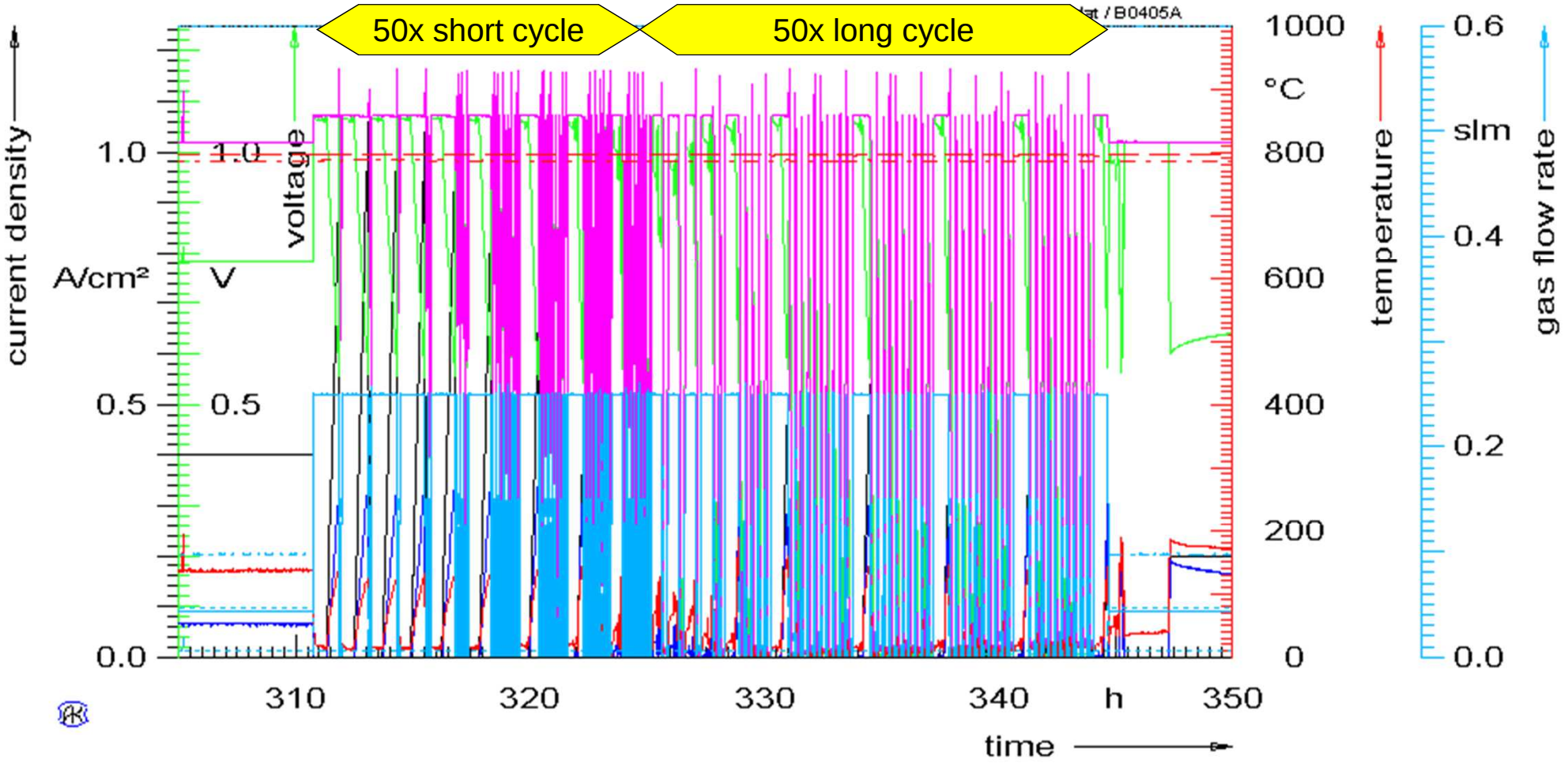

Redox Stability of Electrolyte Supported SOFC

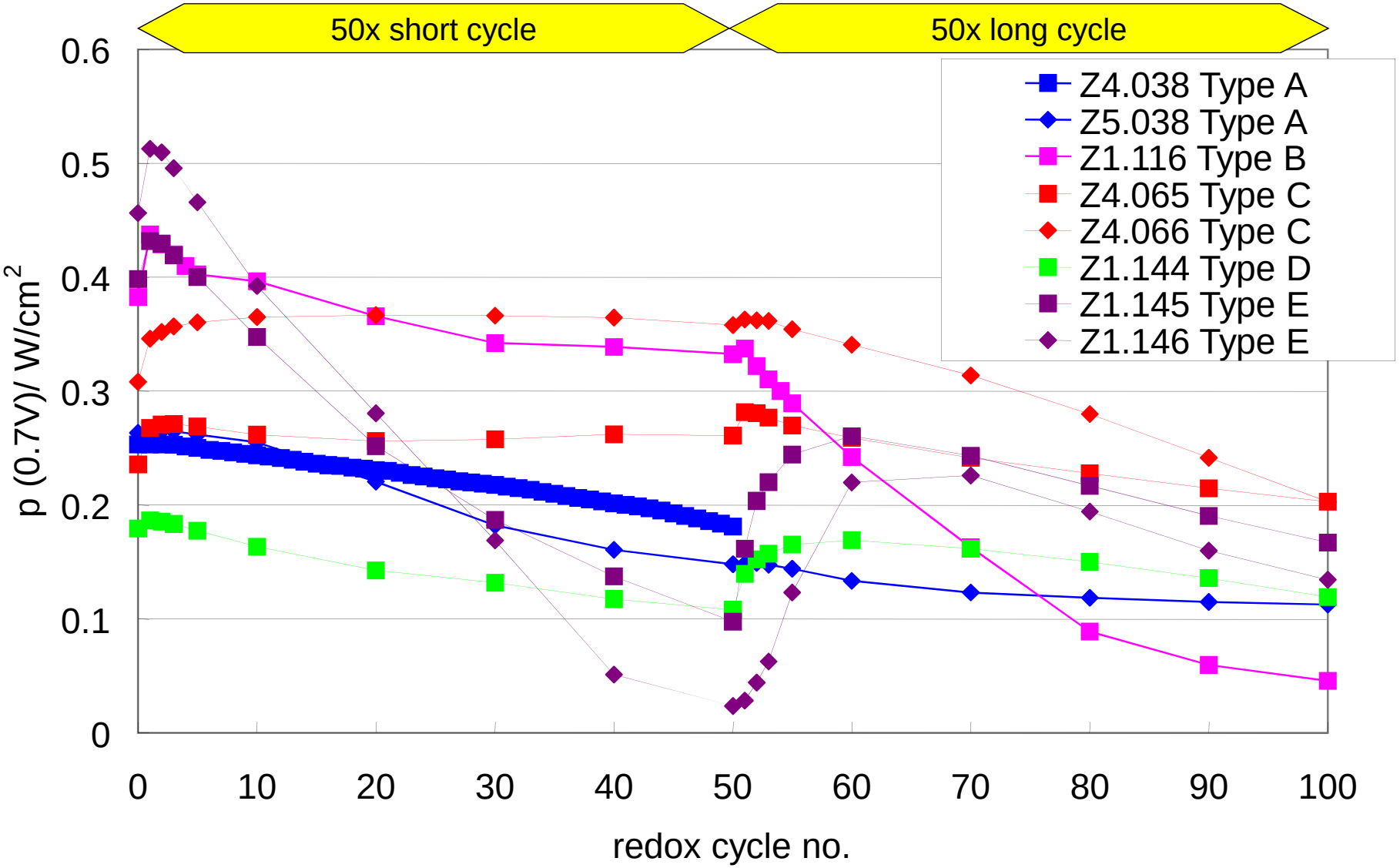

Anode:
Aufkohlung im Betrieb mit C_nH_m

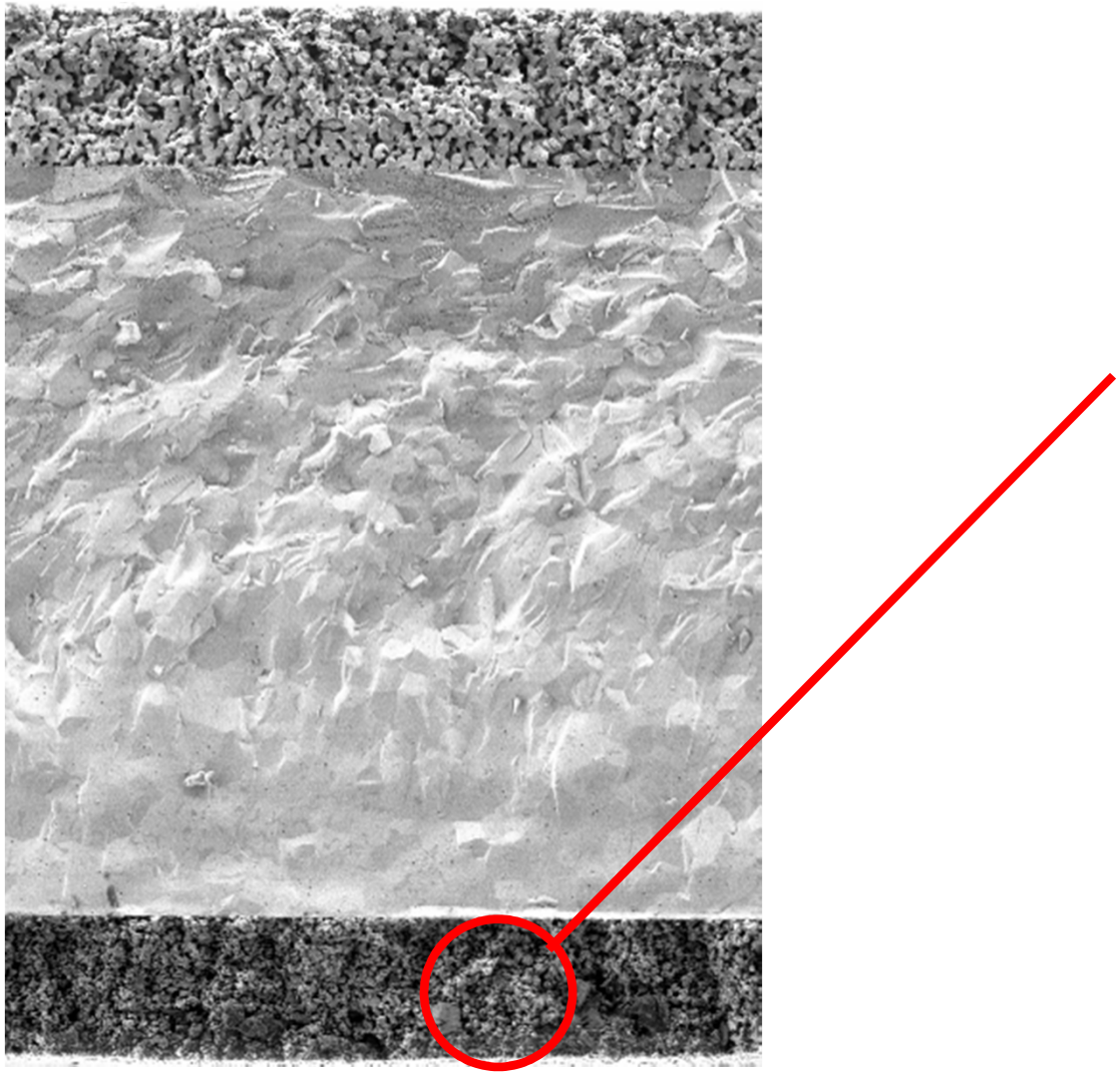

Operation on Hydrocarbons
Severe Degradation with higher Hydrocarbons C_nH_m

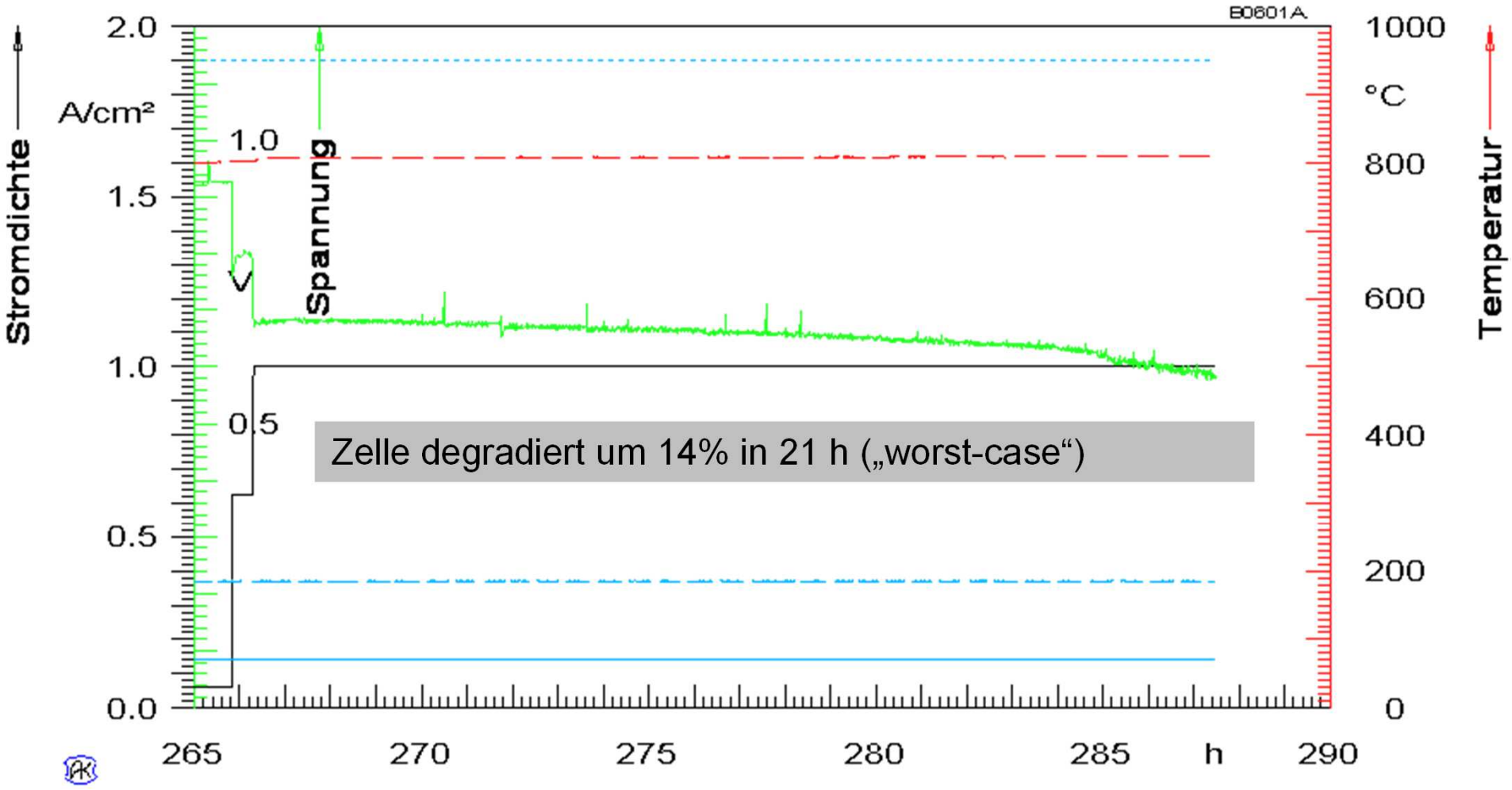

Gasgemisch: H_2, CO, H_2O, CO_2, N_2, C_2H_2 (Ethin), C_7H_8 (Toluol), Methylnaphtalin ($C_{11}H_{10}$)

Operation on Hydrocarbons
Severe Degradation with higher Hydrocarbons C_nH_m

Flussrichtung

Aufgekohlte Zelle nach Betrieb mit einem Gasgemisch bestehend aus aus H_2, CO, H_2O, CO_2, N_2, C_2H_2 (Ethin), C_7H_8 (Toluol) und Methylnaphtalin ($C_{11}H_{10}$)

Kathode:
Alterung im Betrieb mit Lastzyklen

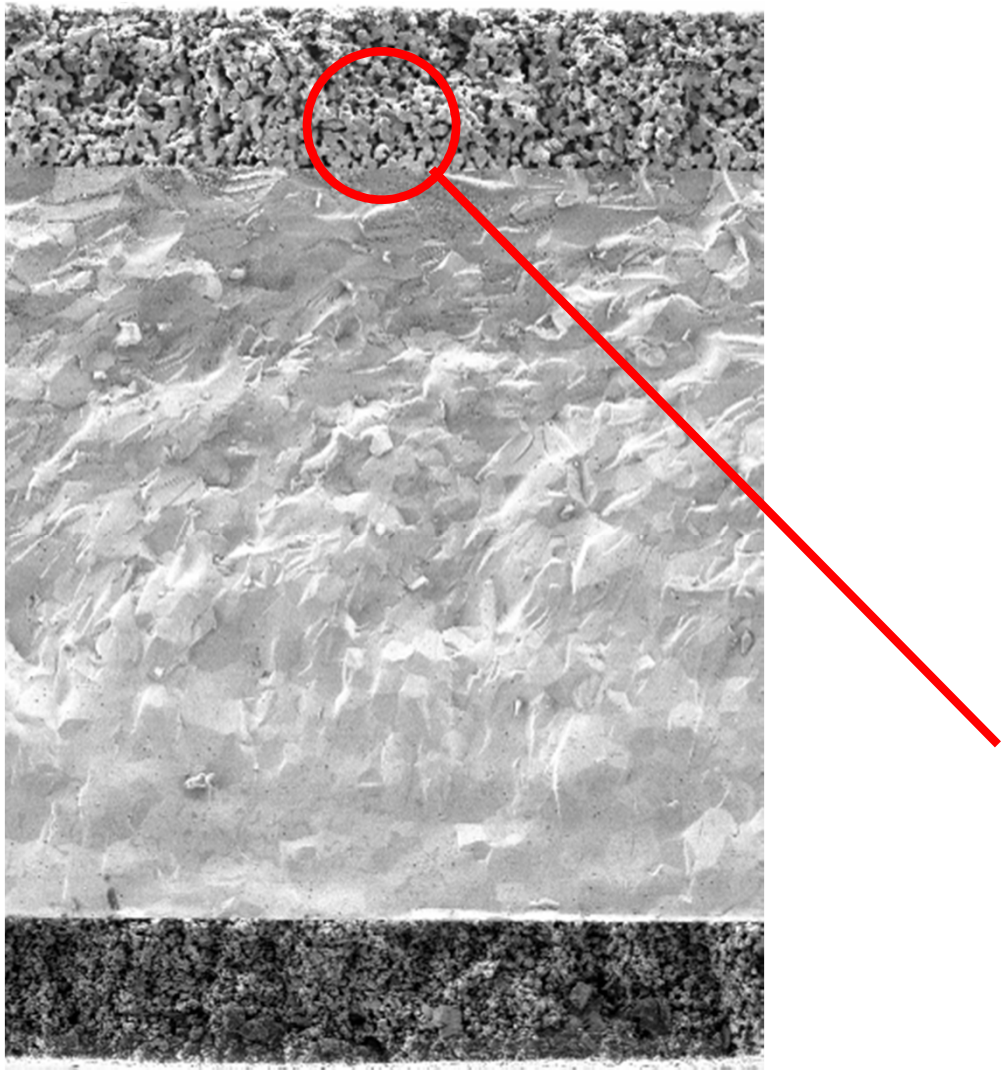

Electrochemical Characterization of Degradation Phenomena
Load Cycling Test (966 cycles within ~ 400 hours)

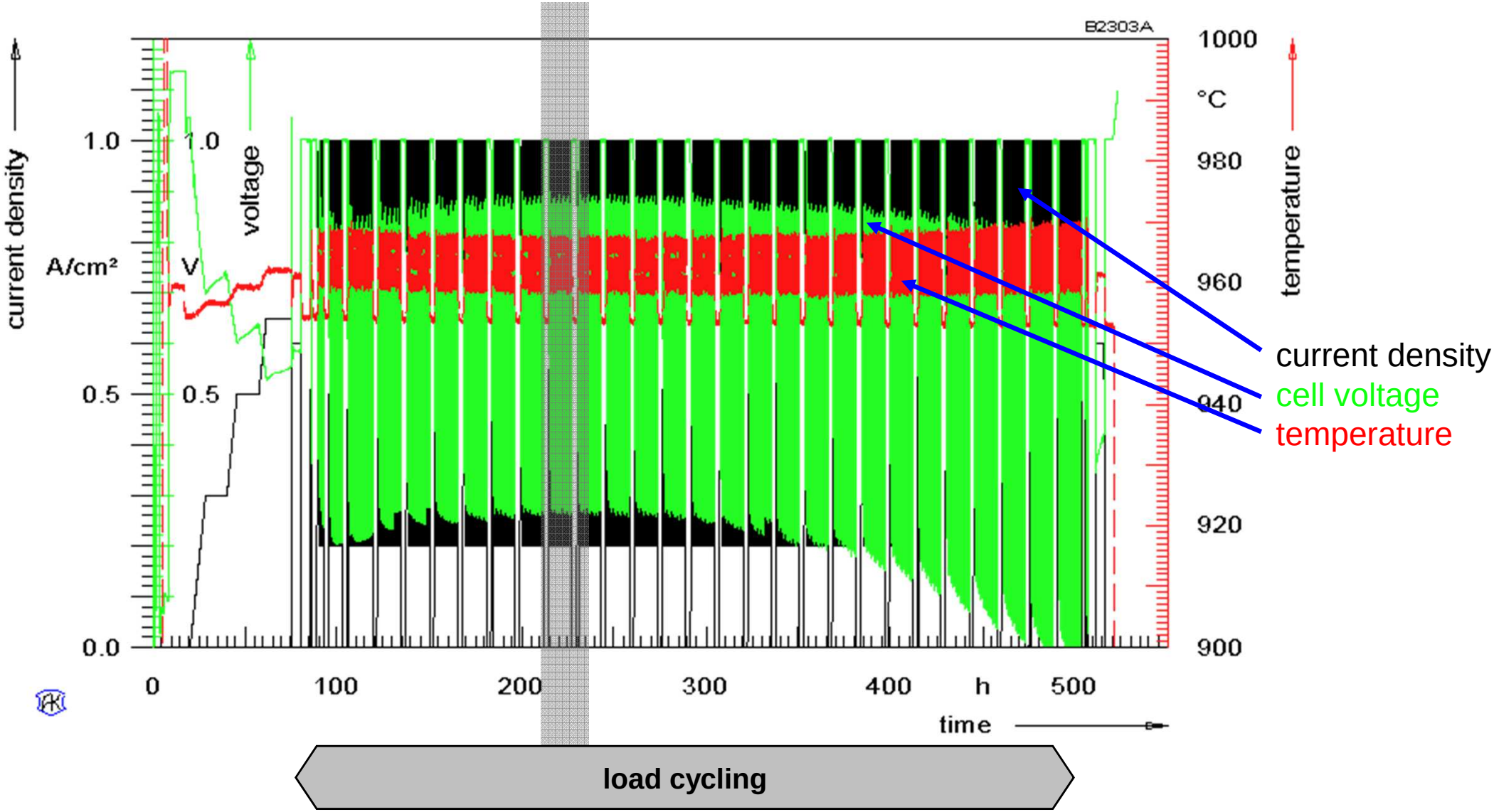

Electrochemical Characterization of Degradation Phenomena
Load Cycling Test

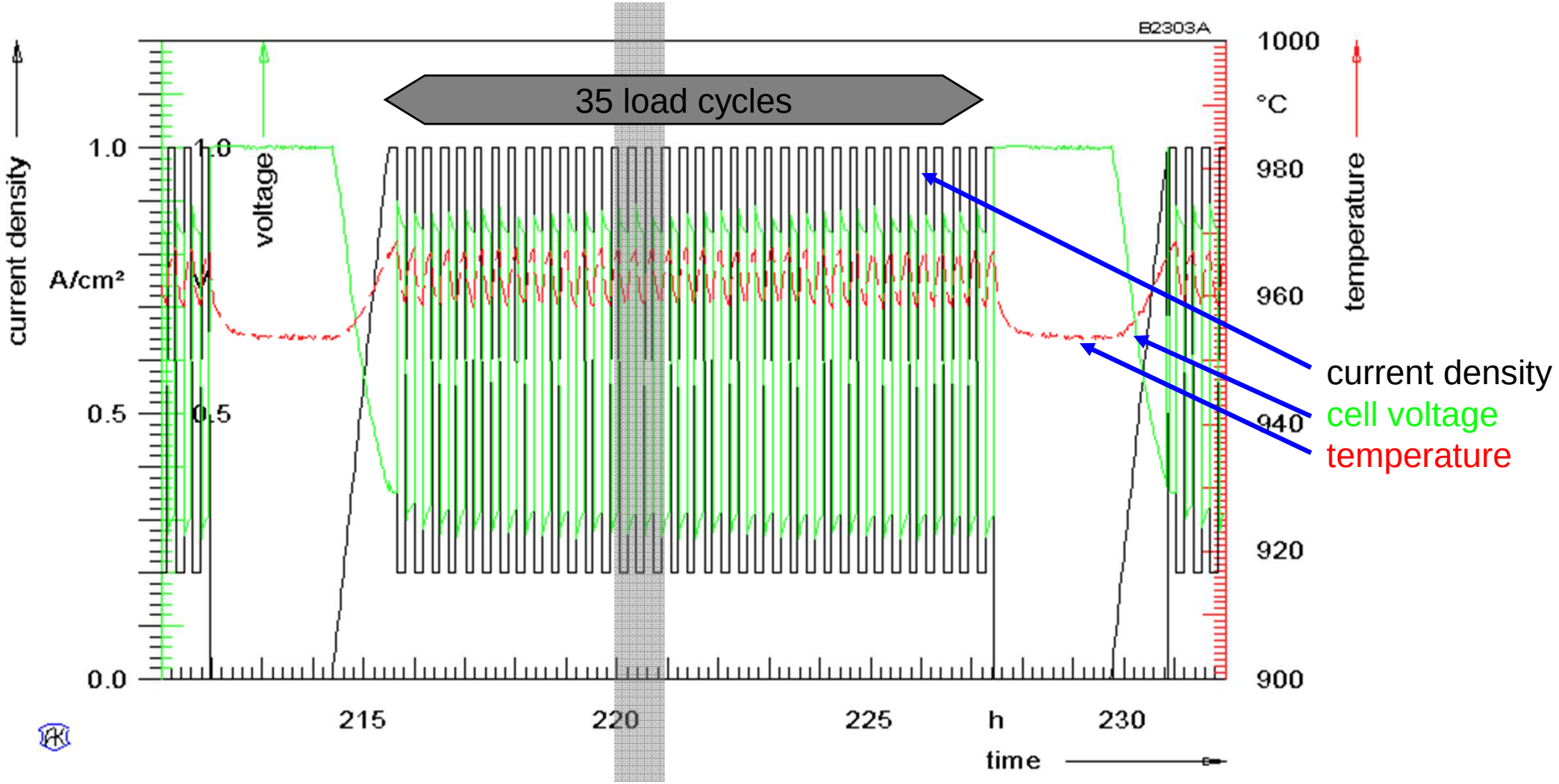

Electrochemical Characterization of Degradation Phenomena
Load Cycling Test

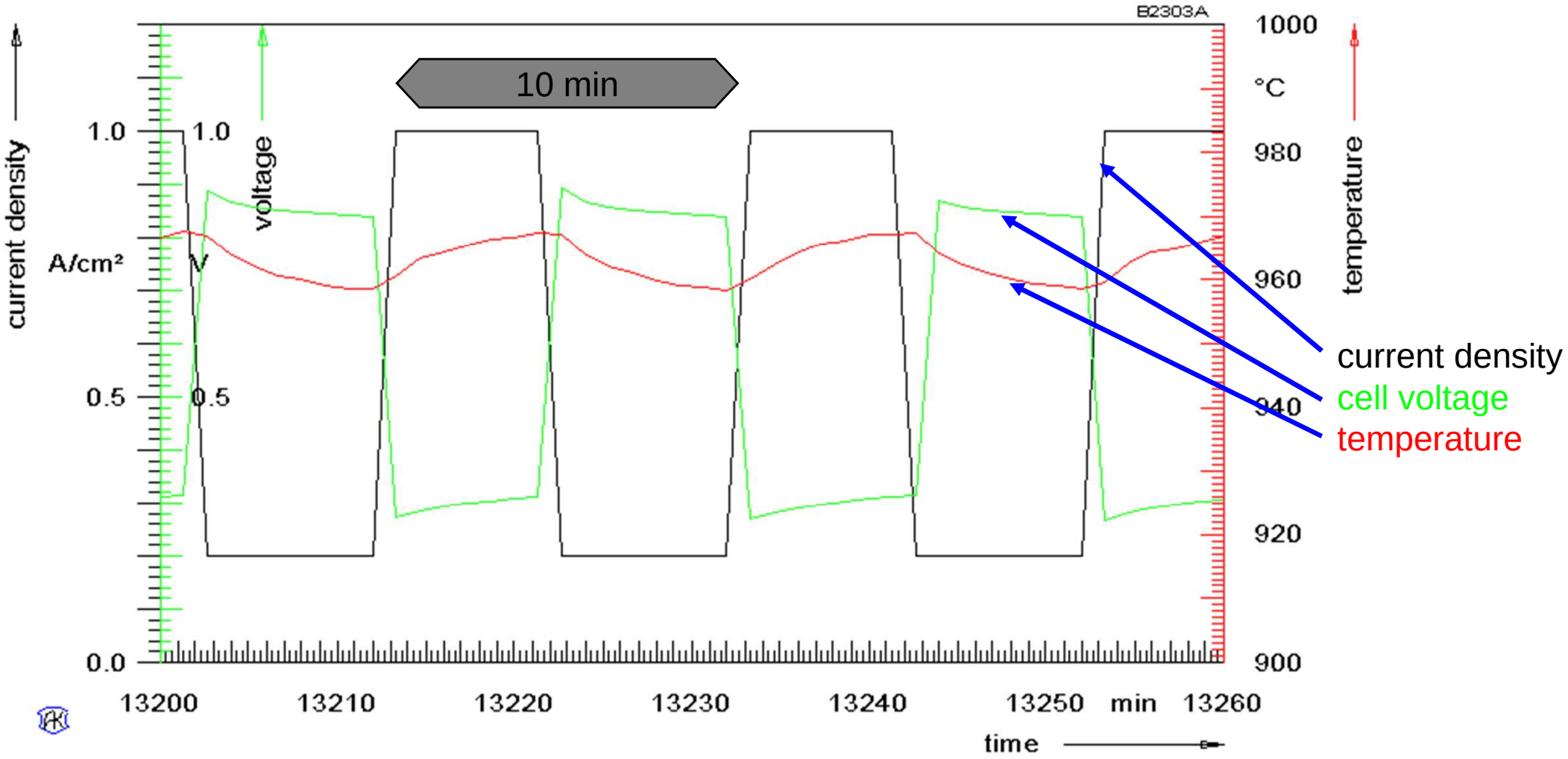

Electrochemical Characterization of Degradation Phenomena
CV-characteristic before and after Load Cycling Test

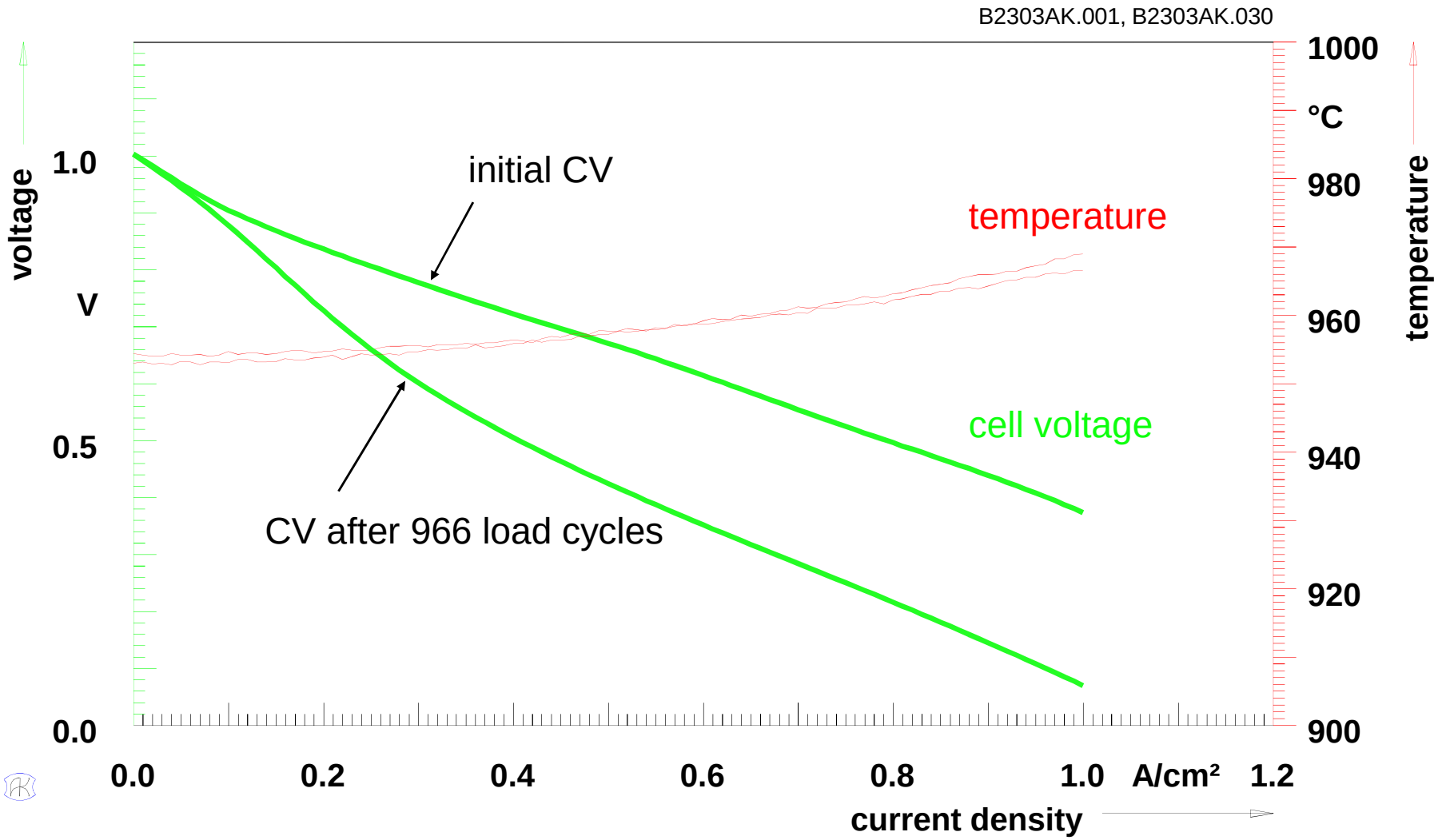

CV: current voltage characteristic

Modeling of Degradation Phenomena
Chemical Potential Diagrams and Thermodynamic Equilibrium Calculations

MALT (MAterials oriented Little Thermodynamic database*)

$\Delta_f G°$, $\Delta_f H°$, $S°$, $C_p°$ at 298.15 K

temperature coefficients of heat capacities, transition temperatures, transition enthalpies

Calculation of Chemical Potential Diagrams
(CHD)

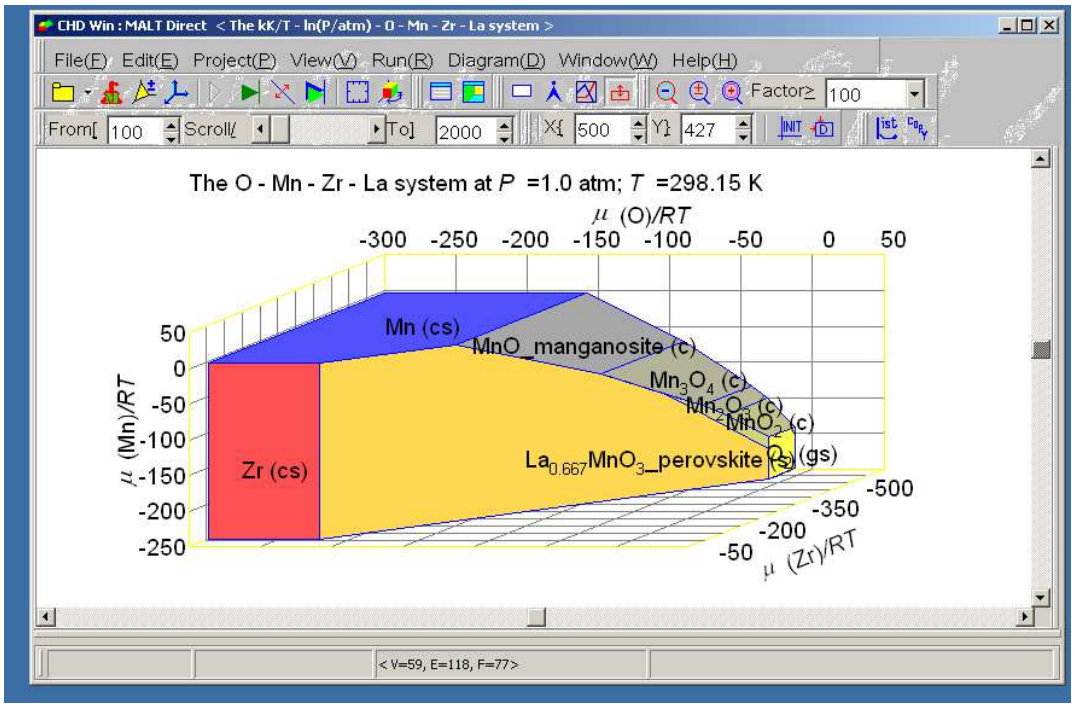

Thermodynamic Equilibrium Calculations
(GEM: Gibbs Energy Minimizer)

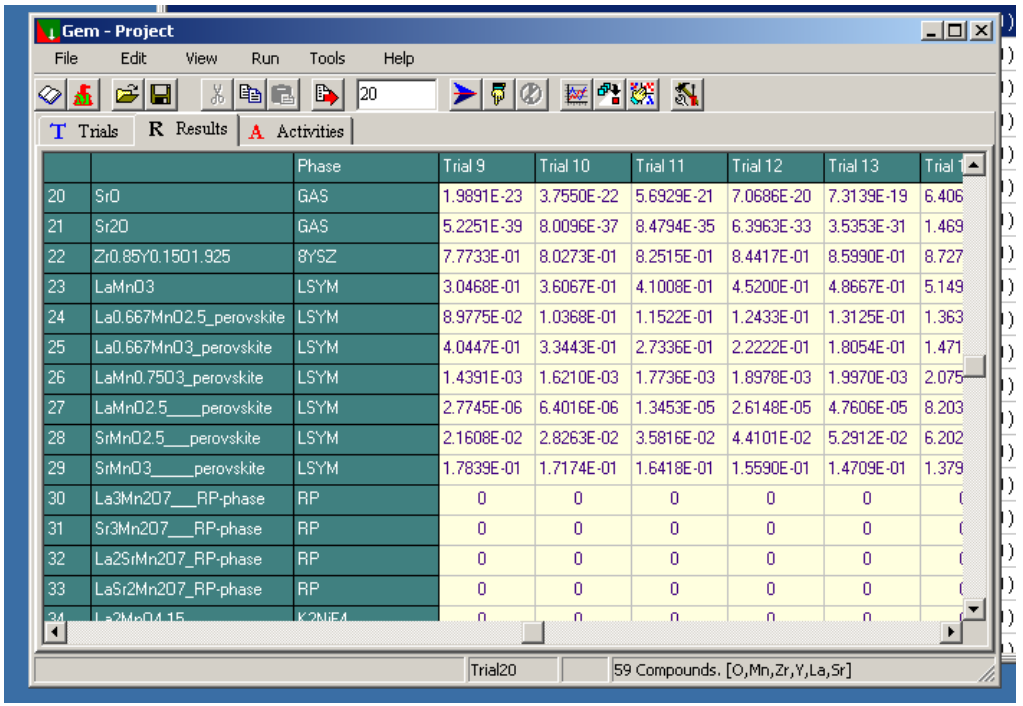

		Phase	Trial 9	Trial 10	Trial 11	Trial 12	Trial 13
20	SrO	GAS	1.9891E-23	3.7550E-22	5.6929E-21	7.0686E-20	7.3139E-19
21	Sr2O	GAS	5.2251E-39	8.0096E-37	8.4794E-35	6.3963E-33	3.5353E-31
22	Zr0.85Y0.1501.925	8YSZ	7.7733E-01	8.0273E-01	8.2515E-01	8.4417E-01	8.5990E-01
23	LaMnO3	LSYM	3.0468E-01	3.6067E-01	4.1008E-01	4.5200E-01	4.8667E-01
24	La0.667MnO2.5_perovskite	LSYM	8.9775E-02	1.0368E-01	1.1522E-01	1.2433E-01	1.3125E-01
25	La0.667MnO3_perovskite	LSYM	4.0447E-01	3.3443E-01	2.7336E-01	2.2222E-01	1.8054E-01
26	LaMn0.7503_perovskite	LSYM	1.4391E-03	1.6210E-03	1.7736E-03	1.8978E-03	1.9970E-03
27	LaMnO2.5___perovskite	LSYM	2.7745E-06	6.4016E-06	1.3453E-05	2.6148E-05	4.7606E-05
28	SrMnO2.5___perovskite	LSYM	2.1608E-02	2.8263E-02	3.5816E-02	4.4101E-02	5.2912E-02
29	SrMnO3_____perovskite	LSYM	1.7839E-01	1.7174E-01	1.6418E-01	1.5590E-01	1.4709E-01
30	La3Mn2O7___RP-phase	RP	0	0	0	0	0
31	Sr3Mn2O7___RP-phase	RP	0	0	0	0	0
32	La2SrMn2O7_RP-phase	RP	0	0	0	0	0
33	LaSr2Mn2O7_RP-phase	RP	0	0	0	0	0

*** H. Yokokawa et al.,Thermochimica Acta 245, 45-55 (1994)**
MALT for Windows, see http://www.kagaku.com/malt/index.html

Modeling of Degradation Phenomena

Chemical Potential Diagram for the polarized LSM / 8YSZ - Interface

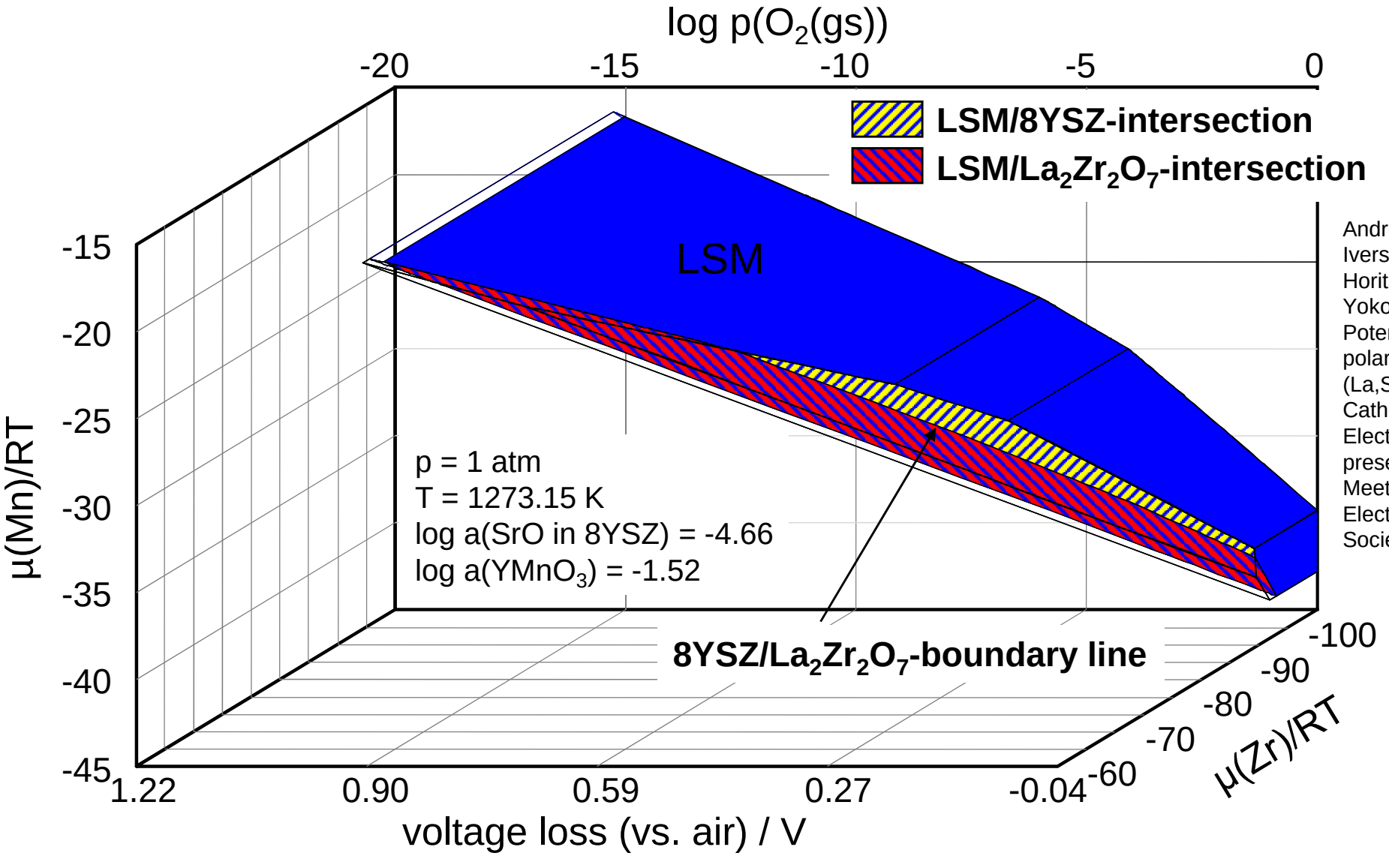

André Weber, Ellen Ivers-Tiffée, Teruhisa Horita, Harumi Yokokawa, Chemical Potential Diagrams for polarized (La,Sr)MnO_3+d-Cathode/8YSZ-Electrolyte-Interfaces", presented at the 206th Meeting of The Electrochemical Society, 2004

Modeling of Degradation Phenomena
Formation of insulating LZO-layers at the LSM/8YSZ Interface

calculated amount of LZO

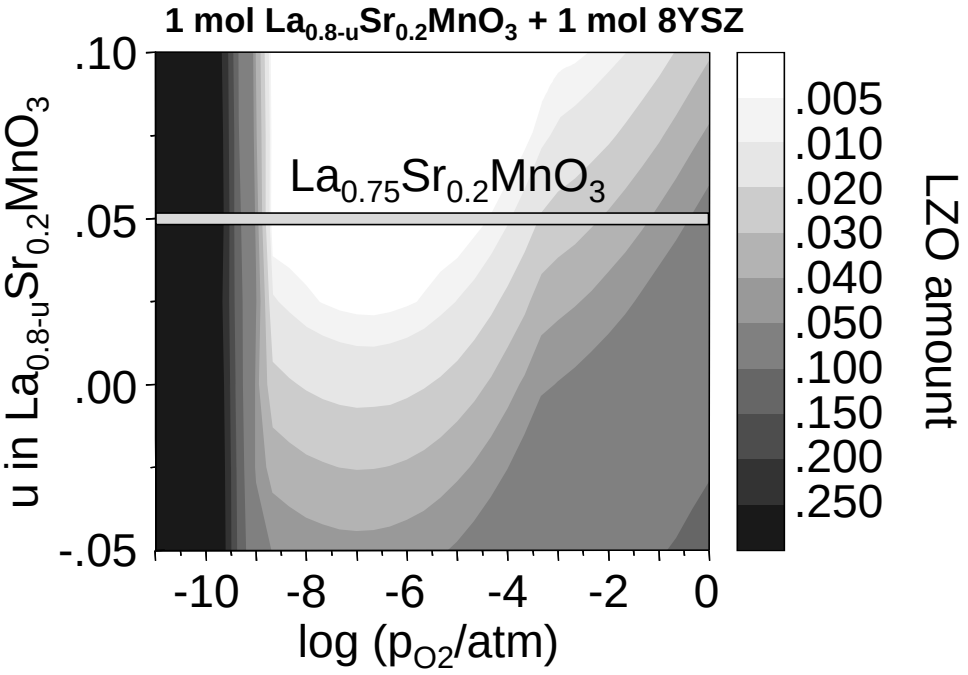

impact of cathode overvoltage η_{cat}

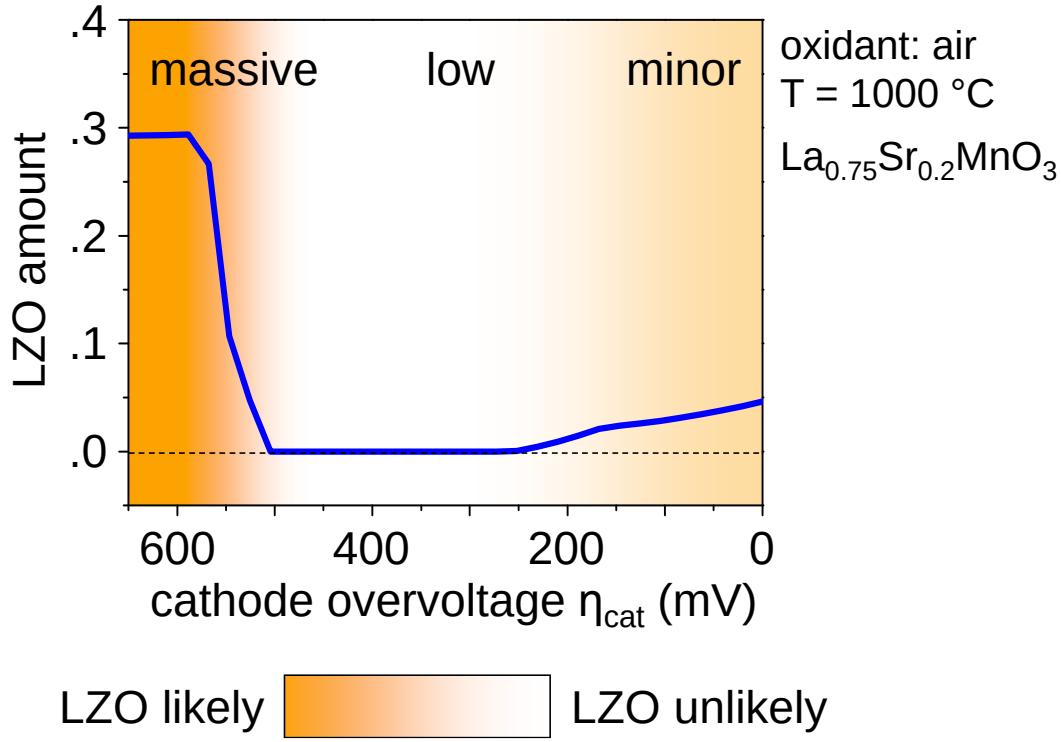

M. J. Heneka, E. Ivers-Tiffée: Degradation of SOFC Single Cells Under Severe Current Cycles. In: S. C. Singhal, J. Mizusaki (Hrsg.), Proc. 9th Int. Symp. on SOFC, PV 2005-07, The Electrochemical Society, 534-543 (2005)

Analysis of Degradation Phenomena
Impact of Load Cycles on LZO-layer at the LSM/8YSZ Interface

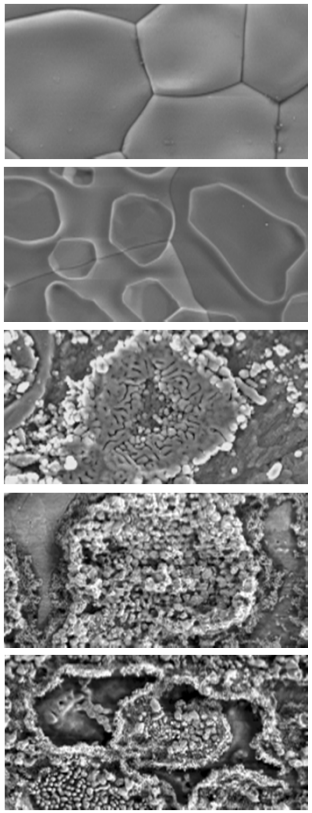

10ScSZ substrate

MEA* sintered at 1300 °C

MEA* activated to 0.65 A/cm²

MEA* 966 cycles, (0.6 ± 0.4) A/cm²

MEA* 434 cycles, (0.6 ± 0.5) A/cm²

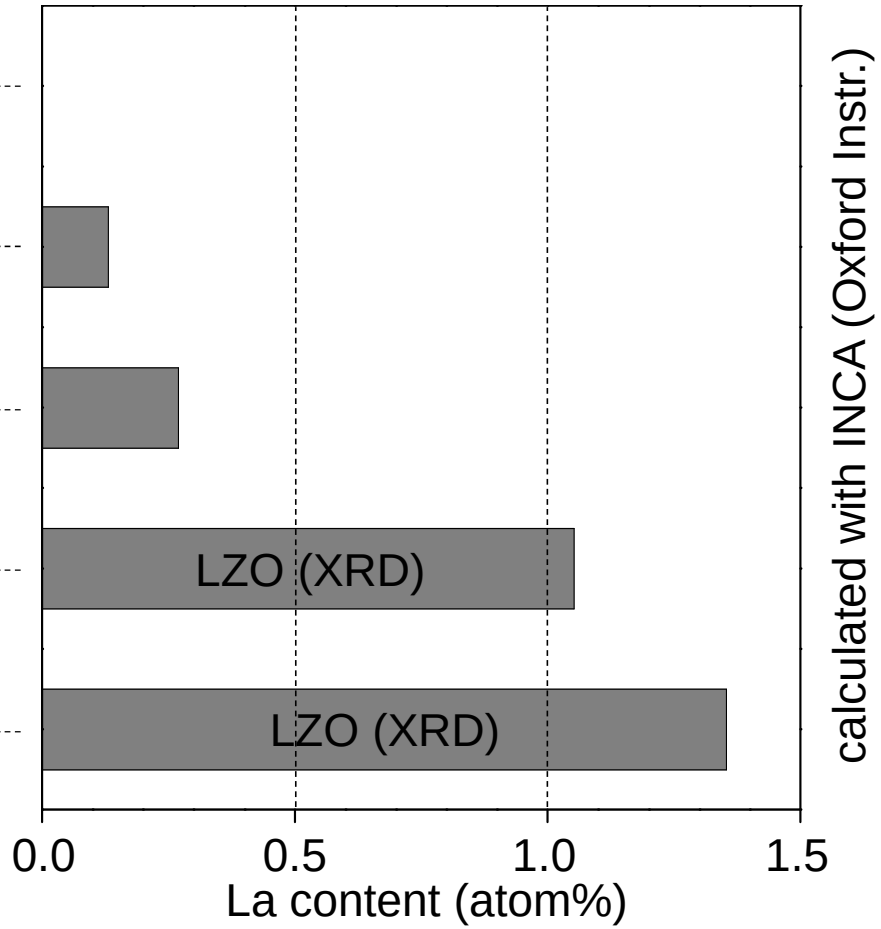

the more intensive the current treatment (amplitude/ cycles), the more the LZO-content increases.

M. J. Heneka, E. Ivers-Tiffée: Degradation of SOFC Single Cells Under Severe Current Cycles. In: S. C. Singhal, J. Mizusaki (Hrsg.), Proc. 9th Int. Symp. on SOFC, PV 2005-07, The Electrochemical Society, 534-543 (2005)

Analysis of Fuel Cell Long-Term Stability
Can we Afford Long-Term Measurements?

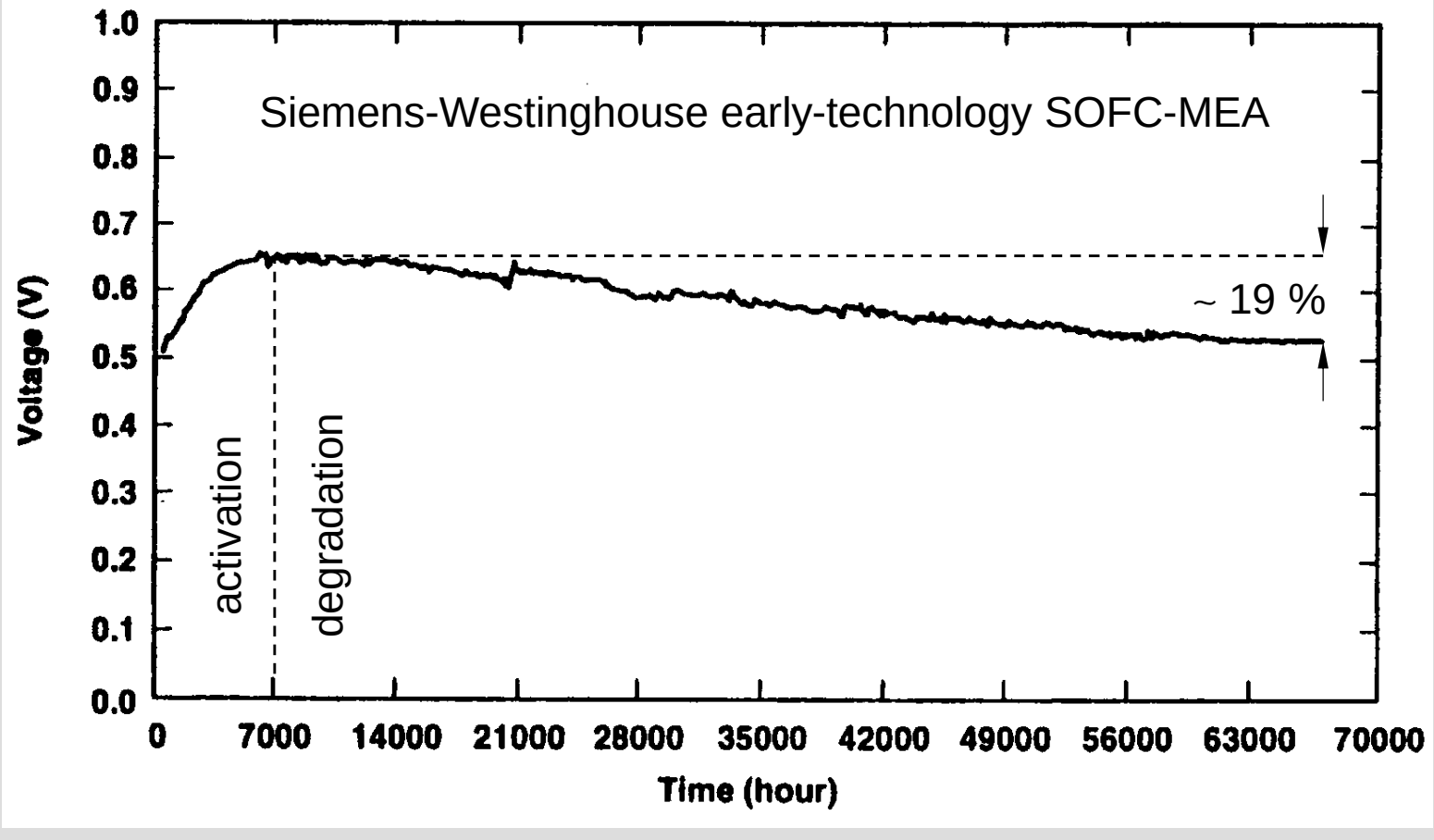

[S.C. Singhal, SOFC V, PV97-40, 1997]

duration
69,000 h
8 years
1989 – 1997

assume
$ 100 per day

cost
$ 300,000 total

degradation
19 % total
0.3 % / 1,000 h

results
available after
5...10 years

MEA: membrane-electrode assembly

Analysis of Fuel Cell Long-Term Stability
Motivation for Accelerated Lifetime Testing

lifetime

lifetime is a critical issue for the success of fuel cells at market.

challenges

- long-term measurements are time consuming and thus expensive.
- if the total damage obtained during long-term test is low, the physical degradation mechanisms are difficult to identify.

possible solution

accelerated life testing (ALT) for fuel cell components and single cells

example: damage during long-term test may be low.

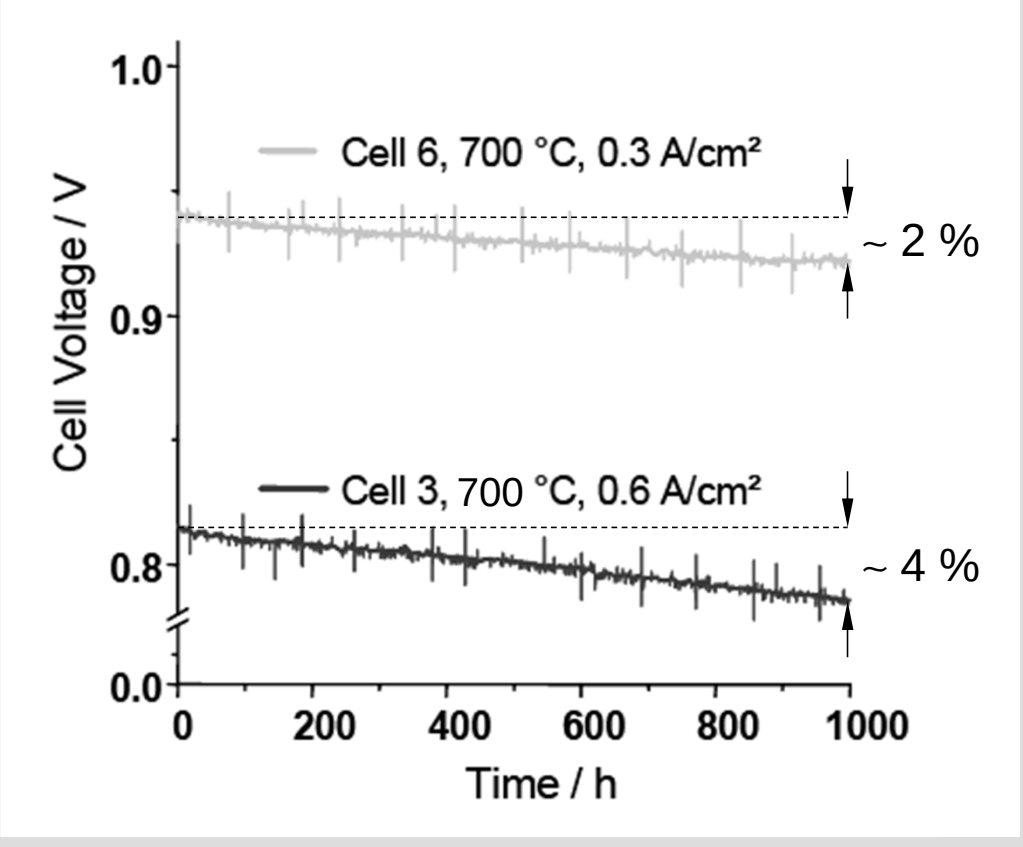

(M. Becker et al., SOFC IX, PV2005-07, 2005)

Basic Concepts in Reliability Engineering
Definition of Failure Event and Time-To-Failure

soft failure

gradual performance loss until (pre-defined) critical level is reached.

example

- voltage/ power degradation in fuel cells

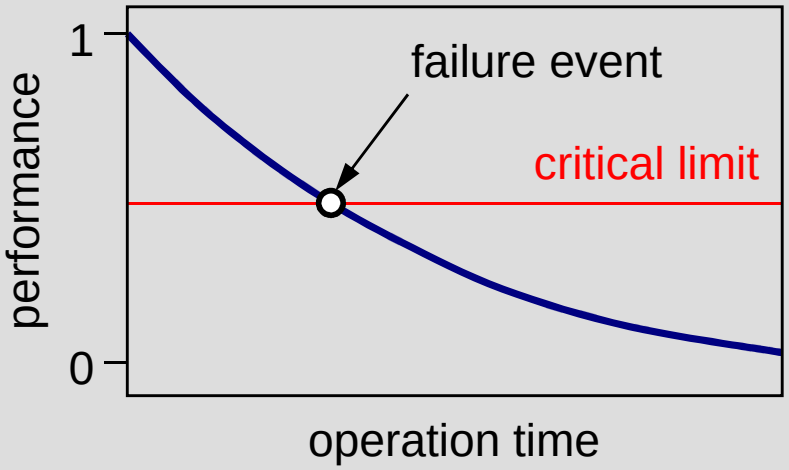

(Meeker et al., Technometrics, 40, 1998)

hard failure

sudden loss of functionality – the device stops working.

example

- light bulb burns out

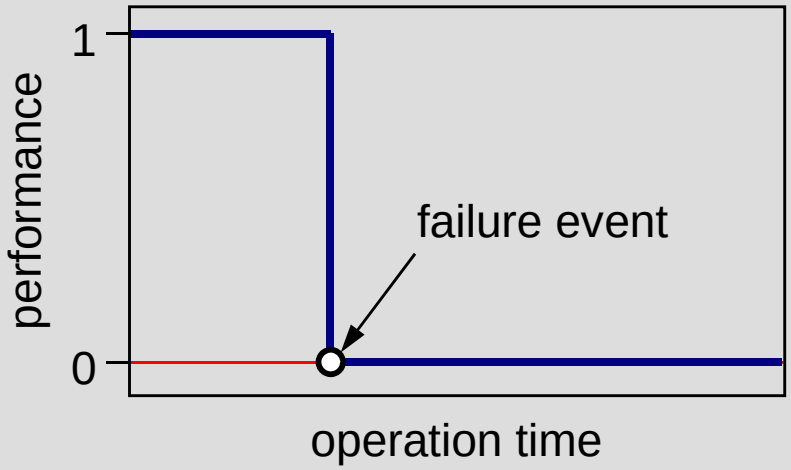

Lifetime and Degradation Assessment
Overview of Life Testing Methods

"conventional" life testing

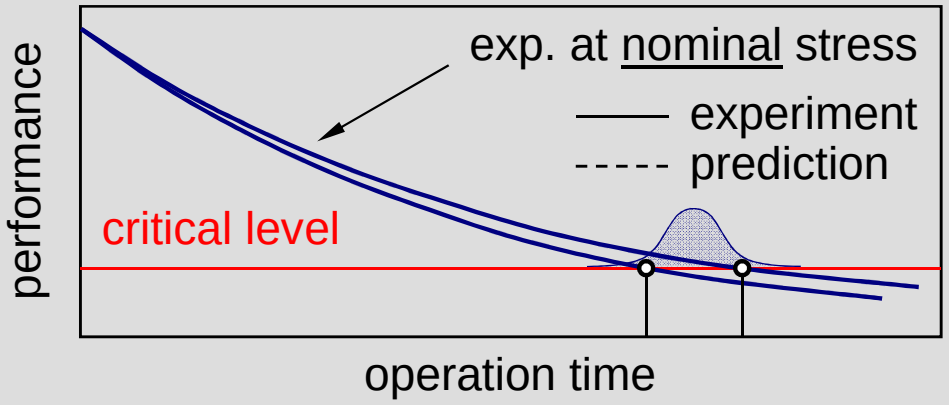

accelerated life testing

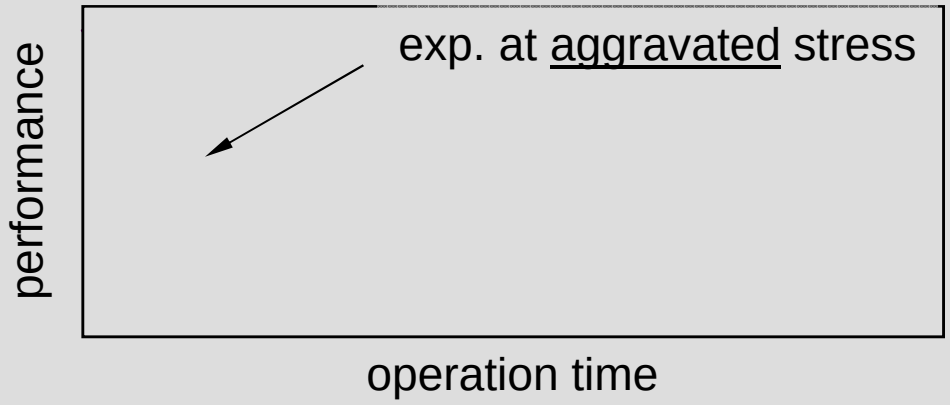

degradation testing

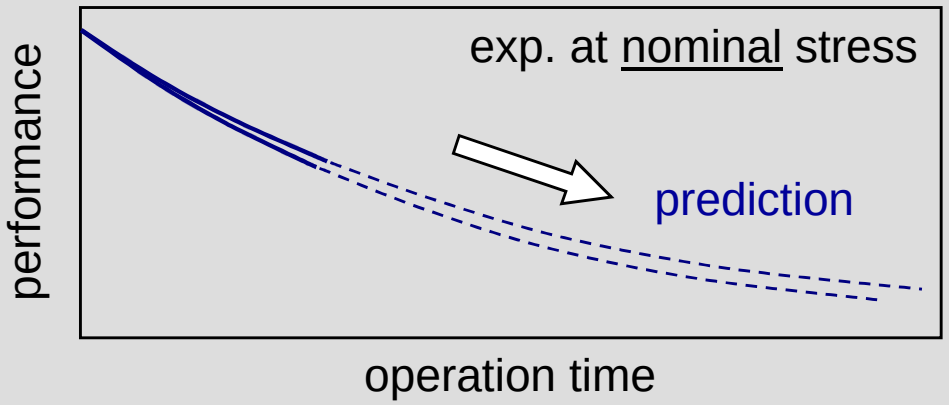

accelerated degradation testing

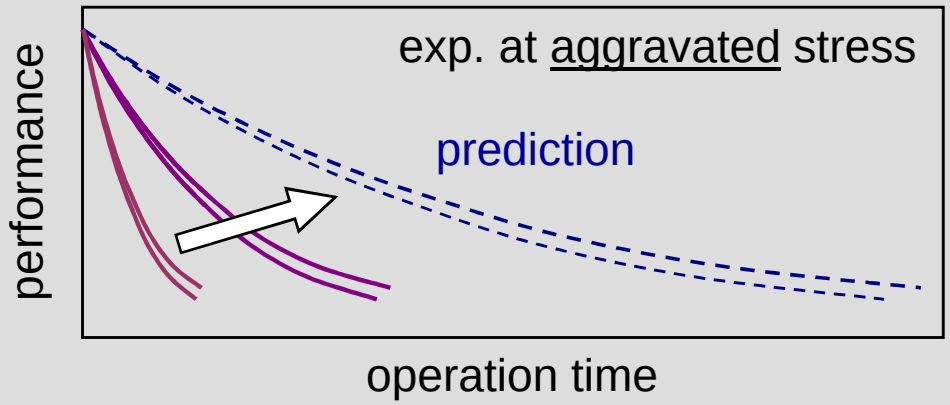

Accelerated Life Testing
Approach and Advantages

approach

- degradation is accelerated by means of aggravated stress (current load, temperature, etc.).
- life-stress relationship is modelled by the use of failure data.
- extrapolation of life-stress model gives a prediction for service life at nominal stress.

advantages

- physical consequences of degradation appear more clearly, mechanisms are identified more easily.
- precious measurement time is saved, lifetime is evaluated rapidly.

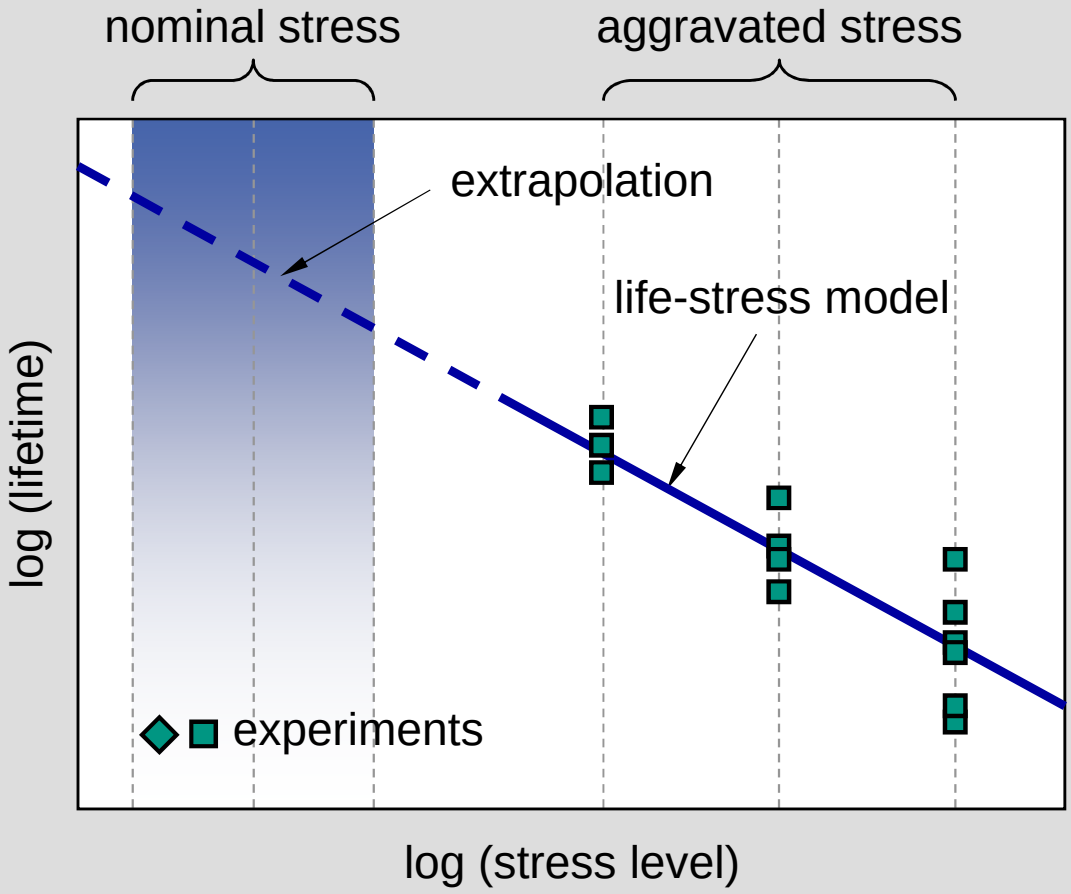

(W. Nelson, Accelerated Life Testing, John Wiley & Sons, 1990)

Accelerated Life Testing
Competing Failure Modes in Accelerated Testing

difficulty

- if there are competing failure modes, accelerated life testing may lead to incorrect statements.

example

- two degradation processes *A*, *B*.
- degradation mechanism *B* is masked by failure mode *A* at aggravated stress levels.
- extrapolation of life-stress model to nominal stress levels will be wrong.

failure mechanisms *A*, *B* need to be separated for correct life modelling!

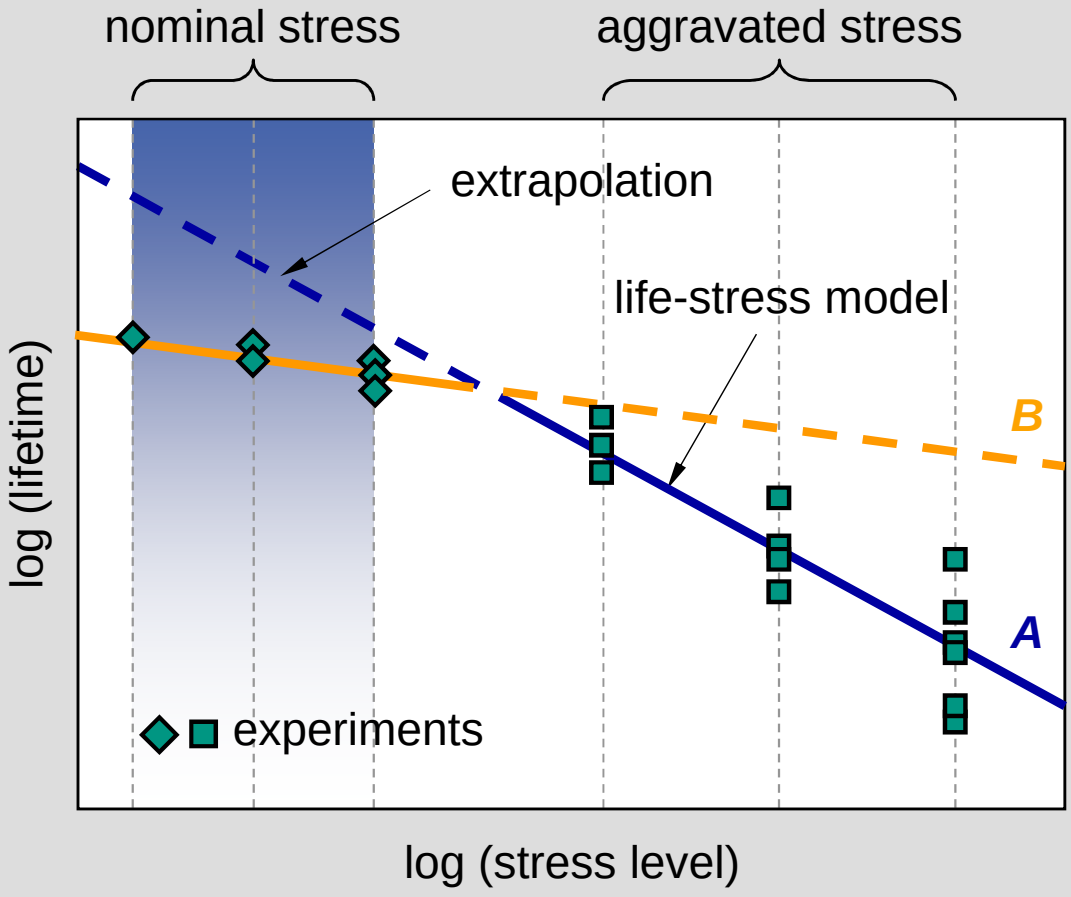

(W.Q. Meeker et al., IEEE Transactions on Reliability, 47, 1998)

Accelerated Life Testing
Competing Degradation Processes in Solid Oxide Fuel Cells

in SOFC

many potentially competing degradation mechanisms are known:

a) delamination of layers
b) agglomeration of catalyst particles
c) formation of secondary phases
d) interdiffusion and demixing
e) densification of porous electrodes
f) carbon deposition in anode
g) electrolyte conductivity loss
h) corrosion of interconnects
i) etc.

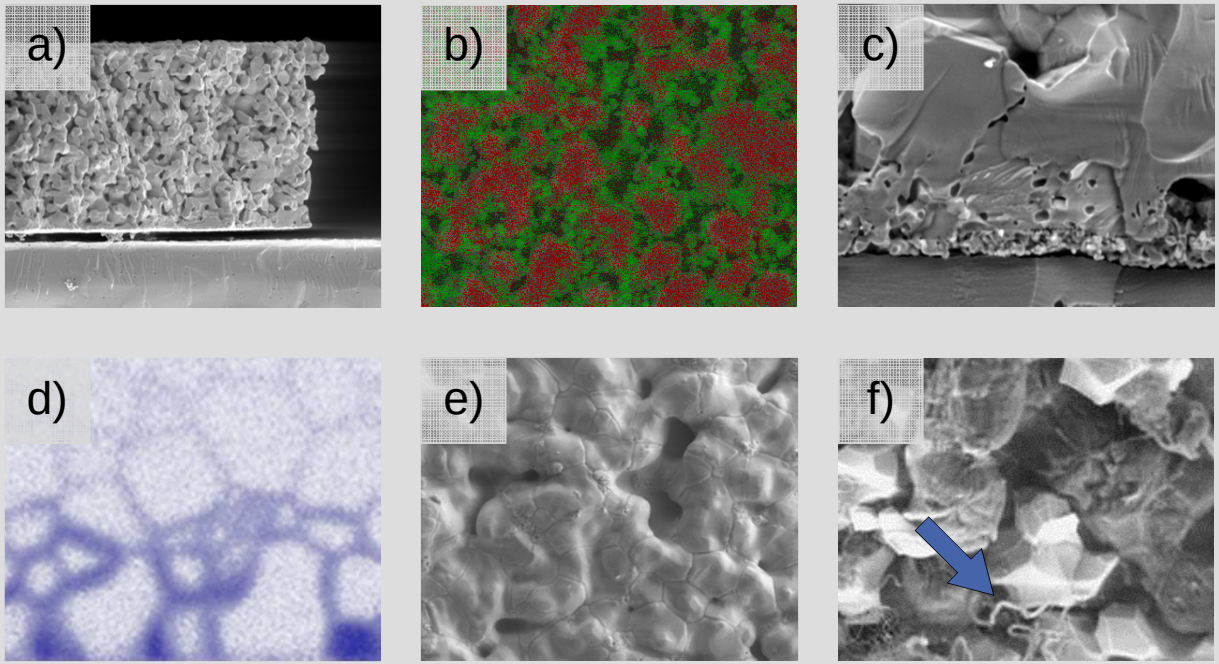

⇨ in addition, activation processes that improve the performance are known (from cathodes).